water

MDPI

Article

Barrier Islands Resilience to Extreme Events: Do Earthquake and Tsunami Play a Role?

Ella Meilianda [1,2,*], Franck Lavigne [3,4], Biswajeet Pradhan [5,6,7], Patrick Wassmer [4], Darusman Darusman [8] and Marjolein Dohmen-Janssen [9]

1 Tsunami and Disaster Mitigation Research Center (TDMRC), Universitas Syiah Kuala, Banda Aceh 23233, Indonesia
2 Civil Engineering Department, Engineering Faculty, Universitas Syiah Kuala, Banda Aceh 23111, Indonesia
3 Geography Department, University of Paris 1 Panthéon-Sorbonne, 75005 Paris, France; franck.lavigne@univ-paris1.fr
4 Laboratoire de Geographie Physique, UMR 8591 CNRS, 1 Place A. Briand, 92190 Meudon, France; patrick.wassmer@lgp.cnrs.fr
5 Centre for Advanced Modelling and Geospatial Information Systems (CAMGIS), University of Technology Sydney, Ultimo, NSW 2007, Australia; biswajeet.pradhan@uts.edu.au
6 Center of Excellence for Climate Change Research, King Abdulaziz University, P.O. Box 80234, Jeddah 21589, Saudi Arabia
7 Earth Observation Center, Institute of Climate Change, Universiti Kebangsaan Malaysia, Bangi 43600 UKM, Selangor, Malaysia
8 Post-Graduate School, Universitas Syiah Kuala, Banda Aceh 23111, Indonesia; darusman@unsyiah.ac.id
9 Water Engineering & Management (WEM), Faculty of Engineering & Technology, University of Twente, 7522 NB Enschede, The Netherlands; c.m.dohmen-janssen@utwente.nl
* Correspondence: ella_meilianda@unsyiah.ac.id

Abstract: Barrier islands are indicators of coastal resilience. Previous studies have proven that barrier islands are surprisingly resilient to extreme storm events. At present, little is known about barrier systems' resilience to seismic events triggering tsunamis, co-seismic subsidence, and liquefaction. The objective of this study is, therefore, to investigate the morphological resilience of the barrier islands in responding to those secondary effects of seismic activity of the Sumatra–Andaman subduction zone and the Great Sumatran Fault system. Spatial analysis in Geographical Information Systems (GIS) was utilized to detect shoreline changes from the multi-source datasets of centennial time scale, including old topographic maps and satellite images from 1898 until 2017. Additionally, the earthquake and tsunami records and established conceptual models of storm effects to barrier systems, are corroborated to support possible forcing factors analysis. Two selected coastal sections possess different geomorphic settings are investigated: (1) Lambadeuk, the coast overlying the Sumatran Fault system, (2) Kuala Gigieng, located in between two segments of the Sumatran Fault System. Seven consecutive pairs of comparable old topographic maps and satellite images reveal remarkable morphological changes in the form of breaching, landward migrating, sinking, and complete disappearing in different periods of observation. While semi-protected embayed Lambadeuk is not resilient to repeated co-seismic land subsidence, the wave-dominated Kuala Gigieng coast is not resilient to the combination of tsunami and liquefaction events. The mega-tsunami triggered by the 2004 earthquake led to irreversible changes in the barrier islands on both coasts.

Keywords: Sumatra; barrier island; earthquake; tsunami; land subsidence; liquefaction; morphology resilience; GIS

Citation: Meilianda, E.; Lavigne, F.; Pradhan, B.; Wassmer, P.; Darusman, D.; Dohmen-Janssen, M. Barrier Islands Resilience to Extreme Events: Do Earthquake and Tsunami Play a Role?. *Water* **2021**, *13*, 178. https://doi.org/10.3390/w13020178

Received: 30 October 2020
Accepted: 8 January 2021
Published: 13 January 2021

1. Introduction

Major earthquakes that have occurred in history have caused fatalities and losses beyond the direct earthquake shaking. Looking at historical losses from 1900 onward,

around 1% of damaging earthquakes in history have caused about 93% of deaths worldwide. Within those events, secondary effects, such as a tsunami, liquefaction, fire, and the impact of nuclear power plants, have caused 40% of economic losses and deaths [1]. Coastal areas situated at the peripheral of tectonic subduction zones, such as the Sunda Trench, Peru-Chile Trench, and Japan Trench, are subject to multiple threats of co-seismic and post-seismic secondary effects. The triggered massive landslides, liquefaction, and tsunami have caused severe casualties and damage to the affected areas. The Central Sulawesi tectonic earthquake in September 2018, for instance, has triggered multiple secondary effects, including localized tsunami, landslides, and liquefaction [2]. The Great Eastern Japan Earthquake in April 2011 triggered the tsunami, liquefaction, fire, and the impact of a nuclear power plant [1]. The Great Sumatran Earthquake in December 2004 triggered both mega-tsunamis and land subsidence, all of which have caused significant fatalities and losses and required long-term recovery.

Eighty percent of the world's coasts are rocky [3], characterized by a sedimentary-deficit, and a complex morphology [4]. On the basis of satellite inventory, Stutz and Pilkey [5] reveal that 20,783 km of shoreline are occupied by 2149 barrier islands worldwide, which is 37% longer than formerly thought. Indonesia is an archipelagic country with an estimated 91,363.65 km of coastline [6], making it the second longest coastline in the world after Canada [4]. The Indonesian archipelago has 44 barrier islands, which equals 2% of the global figure. Their distribution is strongly related to sea-level history in addition to the influence of tectonic settings. Administratively, 80% of districts and municipalities in Indonesia are situated at the coastal areas, making the coastline the multi-purpose zone in the daily life and socio-economic development of the archipelagic nation.

The shoreline along the Sumatra island of Indonesia mostly consists of shore-parallel lagoonal ecosystems separated by chenier-type barrier islands, with crest height on average no more than 2 m [7]. In the temperate zone, such as in the United States, barrier islands are under tremendous pressure of rising sea level and increasing storminess. On the other hand, the barrier islands and beach ridges located in a tectonically active coastal region, such as the entire length of the west and north Sumatra of Indonesia, are equally under tremendous pressure of the potential tsunami, co-seismic and post-seismic land level changing, and liquefaction as the secondary effects of the tectonic fault and subduction earthquakes.

Studies about the influence of the secondary effects of tectonic activities on the barrier island and spit morphological development are currently relatively limited. This study aims to investigate the morphological resilience of the barrier islands in responding to tsunamis, co-seismic subsidence, and liquefaction. Spatial analysis was utilized to detect shoreline changes from the multi-source datasets of the multi-decadal time scale, including old topographic maps and satellite images from 1898 until 2017. As the next step, we identified the history of major or moderate earthquakes that occurred in each consecutive period. Subsequently, we corroborated those earthquake events with the reported impact of the earthquakes on the coastal areas. We also utilized the established conceptual models of storm effects to barrier systems to interpret possible controlling factors causing the remarkable morphological changes observed at two selected coastal sections. The results will be substantial in building a conceptual foundation for interplaying seismic-related forcing factors with the littoral transport regime that determines the morphological resilience of a coastal area.

1.1. Impact of Earthquakes on Coastal Systems

Investigation of a massive earthquake event has always been appealing for scientists. It is the opportunity to improve the understanding of various factors resulting in casualties and damage. Short-term responses of coastal morphology to tsunamis have been widely discussed in the previous studies through various approaches. Some works have combined models of tsunami wave propagation and inundation, and spatial analysis of the damage in the tsunami-affected area [8–10]. Others focused on the geomorphological [11–14], or ecological [10,15] impacts of the tsunami. Additionally, a few tens of meters of land subsi-

dence were also observed as the immediate response of coastal areas to seismic activities was observed early after the occurrence of the megathrust earthquake of December 2004 along the north and west coast of Sumatra Island [16–19]. An extended period investigation to the post-tsunami coastal recovery in Aceh has also been conducted, including further monitoring on changes of shoreline position and land-level changes [20–22], of land use [23], and the vulnerability and living condition of the coastal inhabitants [8,24].

Liquefaction has yet to be discussed thoroughly, concerning the impact of the megathrust 2004 Sumatra earthquake in Banda Aceh. Nevertheless, some indication of liquefaction indeed observed in Port Blair, the capital city of the Andaman and Nicobar Island of India, where various types of buildings, particularly of the typical reinforced concrete ones, have experienced settlement [25]. Such building failures by settlement were also observed and reported in Banda Aceh [26]. Recently, the soil mechanism of the liquefaction potential in Banda Aceh city after the earthquake was evaluated by [27] using the semi-empirical Idriss Method to quantify the liquefaction potential. The result suggests that most of the highly built subdistricts in Banda Aceh are prone to liquefaction. It is noteworthy that the liquefaction impact is not only triggered by the shaking from the megathrust Sumatra–Andaman earthquakes but also potentially by the activation of the Great Sumatran Fault System [28].

Following the megathrust Sumatran earthquake and tsunami of 26 December 2004, a series of geodetic monitoring campaigns were conducted between 2005 and 2015, to monitor the development of the land-level changes of the west coast of Aceh since the 2004 tsunami [21]. The results showed that after experiencing abrupt co-seismic subsidence, the beach experienced uplift with a rate of 27 mm/year since late 2005. This number is an order of magnitude higher than the rate of eustatic sea-level rise, which is around 4–12 mm/year at the Indonesian waters [29]. The results demonstrate a possible relationship between the development of the new frontier beach ridge, the immediate co-seismic land subsidence, and the probable post-seismic rebound (uplift) associated with the viscoelastic mantle relaxation a few years following the mega earthquake.

Overall, the previous studies suggest that the secondary effects of seismic activity, either associated with the off-shore megathrust subduction or mainland tectonic faults activity, play a crucial role in altering the morphological development of the tectonically active coastal area.

1.2. Barrier Islands and Spits Morphological Resilience

Several studies of large barrier systems, including barrier island or beach ridges and sand spits, have been well-studied, primarily when associated with extreme storm events [30–35]. They have shown to constitute a valuable archive of coastal evolution and their morphology, and internal structures contain information on both past relative sea levels and past storminess activity. Barrier islands and sand spits are considered exemplars of coastal resilience [30,31] and critically essential ecosystems to protect the low-lying area behind them [36]. Under the influence of storms, large barrier systems, such as barrier island and beach ridges, are inherently resilient landforms as long as they can internally recycle sediment to maintain overall landform integrity [37], the rate of sea-level rise is not excessive, and there is no sediment deficit [38]. Nott et al. [33] suggest that the building of beach ridges is being slowed down by a decrease in sediment supply to the coast due to less frequent river floods during periods of reduced storminess. While during a storm event barrier islands may experience breaching due to the intensive funneling of the overwash flows into specific throats [39], a calmer wave regime promotes littoral drift, allowing sand spits to grow extensively [30].

Arguably, a tsunami event may contribute to the geomorphological imprint in the evolution of a tectonically active coast in a way similar to a major storm event. Despite different sources and mechanisms, the effect of the destruction caused by a tsunami may have been analog to that of a storm surge, in particular along the coastline, where barrier islands are the first line of natural coastal protection. Studies of short-term shoreline changes of barrier islands at Banda Aceh coast of Sumatra Island, Indonesia after the 2004

tsunami [13], and those at the Dauphin Island, US after the Hurricane Katrina in 2005 [40] are two comparable studies which demonstrated similar variability of shoreline changes caused by extreme events.

Despite the great diversity of storm mechanisms that strike coastal areas, we consider that the impact of the surging waves to barrier islands is equivalent to that of tsunamis. Sallenger [35] identifies four types of storm regimes and how barrier islands respond to those different forcing magnitudes, which later were re-described in detail by [34]. The four regimes are briefly described in [32] which consist of the "Swash regime", "Collision regime", "Overwash regime", and "Inundation regime," which involve the morphological effects of migration, escarpment, breaching, and submergence of the barrier islands, respectively. The case of sinking effects due to co-seismic subsidence or liquefaction is relatively easy to observe by identifying the narrowing subaerial parts by comparing a pair of maps or satellite images of consecutive years. However, it is almost impossible to determine the cause of the sinking by solely relying on the spatial analysis from the multi-temporal maps and satellite images. Therefore, we also corroborate the results from previous studies and the other sources of information and accountable reports to support the analysis.

Successful coastal management that includes mitigation of possible negative impacts must be based on an understanding of these patterns of change as natural responses to high-intensity events [41]. It is also essential to understand the coastal geomorphic setting and the geological boundaries before attempting to model the large-scale behavior of these types of coastal systems [42]. Herein, historical data inevitably play a major role in identifying any remarkable, even more so, the irreversible changes in the long-term past.

2. Study Area

We investigate morphological changes of the seaward-most barrier islands and spits along the coastline of the north tip of Sumatra Island, which is situated between 05°16′15″ N and 05°36′16″ N, and between 95°16′15″ E and 95°22′35″ E (Figure 1a,b). The low-lying coastal area behind them is where the capital city of Aceh Province, Banda Aceh situated in the central part, and surrounded by the Aceh Besar district occupying ca. 125 km^2 northern valley of the Barisan mountain range at the north tip of Sumatra Island, Indonesia. The Barisan mountain range is formed as the backbone of the leading-edge Sumatra Island, parallel to the Great Sumatran Fault running parallel with the Sumatra-Andaman subduction zone, or also known as Sunda Trench (Figure 1a). The shoreline stretches ca. 25 km connecting Ujong Pancu headland in the southwest and the Ujong Batee headland in the northeast (Figure 1c). The brackish back-barrier wetland ecosystem, aquacultures, and lowland coastal villages occupy the area of ca. 4 km width from the coastline with elevations are varying of −0.5 m to +2.0 m from the mean sea level. The entire coastal area was severely devastated by the megathrust earthquake of M 9.0, followed by the gigantic tsunami event on 26 December 2004.

The tsunami disaster caused severe casualties and damaged properties, as well as erosion at the coastline, altering the functionality of the ecosystems and the livelihoods of coastal communities [44]. In Banda Aceh, the shoreline retreated as far as ca. 200 m inland, and erosion rates of 30 m^3/m on average (up to 80 m^3/m locally) were calculated [11]. Six months after the tsunami, the shoreline experienced about 15% further retreats from the initial erosion by the tsunami [13].

Major infrastructure, e.g., port basin, coastal revetments, and coastal roads, collapsed or were destroyed, whereas the coastal environment was also profoundly altered [8]. A comparison of a coastal revetment of before and after the 2004's tsunami at Lambadeuk is depicted in Figure 2a,b, respectively. The remnants of the same revetment were stranded offshore after the disaster event (Figure 2b), suggesting the occurrence of local land subsidence. Several preliminary studies suggest that the local land subsidence at Lambadeuk and Ulee Lheue (Figure 1c) was less than 50 cm [16,18]. On the other hand, the barrier islands which used to protect the built areas behind the Kuala Gigieng coast were breached at their weakest sections by the tsunami waves. Figure 2c,d exemplify one of the breaching

sections of the barrier island at Kuala Gigieng on the fourth day and six months after the tsunami, respectively.

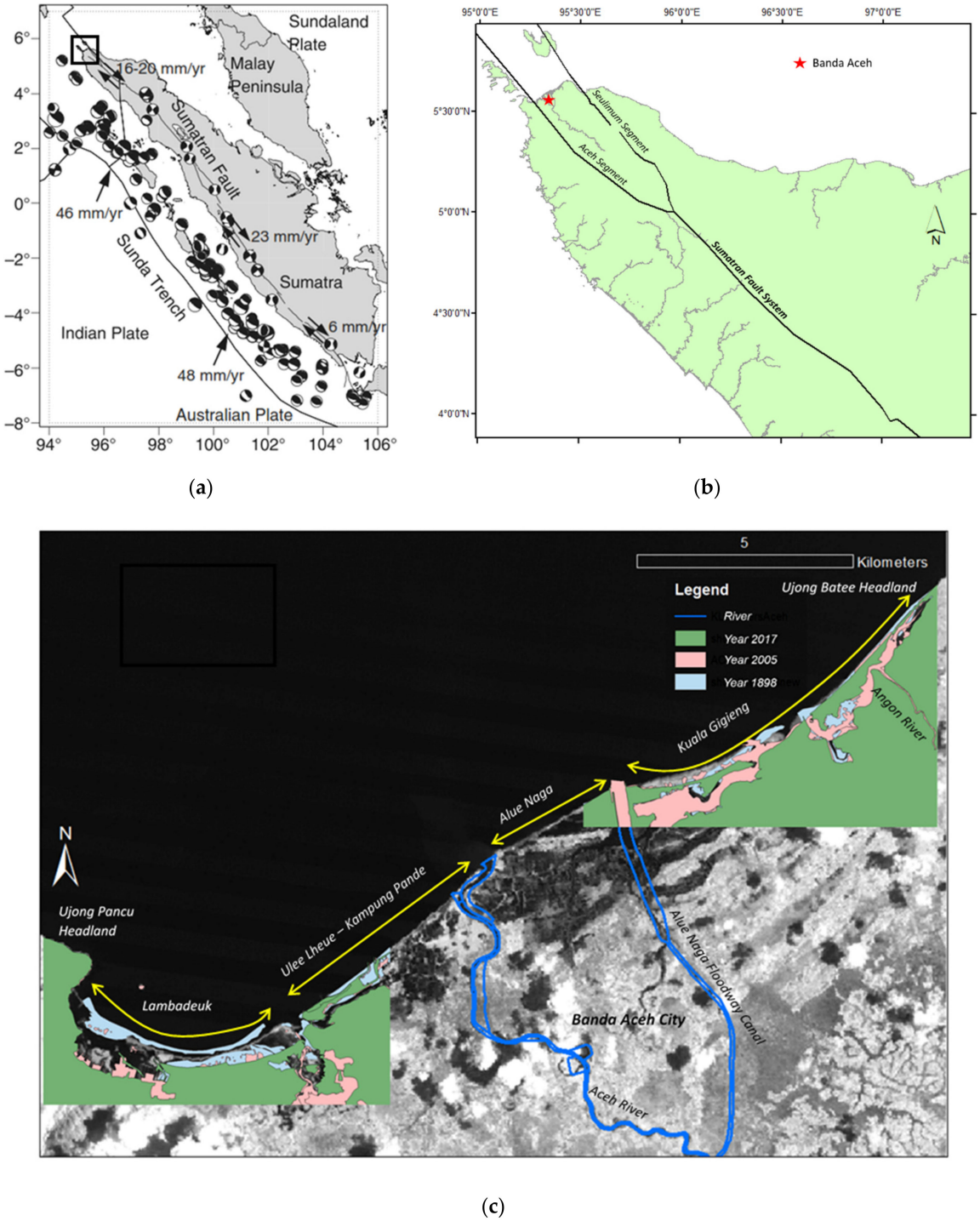

Figure 1. Banda Aceh coast, at the northern tip of Sumatra Island, Indonesia: (**a**) Tectonic settings of Sumatra, compiled from various sources by Hurukawa et al. [43], showing the configuration of the Sumatran fault, slip rates, the plot of Global Centroid Moment tensor (CMT) solutions of shallow earthquakes ($M_w \geq 6.0$ and depth ≤ 60 km) between 1976 and 2012; (**b**) Segments of the Great Sumatran Fault System at the northern Sumatra consists of two bifurcated fault segments, i.e., Aceh Segment and Seulimum Segment. The rectangle shows the investigated coastal area in front of Banda Aceh, the capital of Aceh Province, which is situated between the two fault segments; (**c**) The two investigated coastal sections in this study are Lambadeuk at the southwest and Kuala Gigieng at the northeast since they are the most dynamic and there is less interference by hard-structure coastal protection.

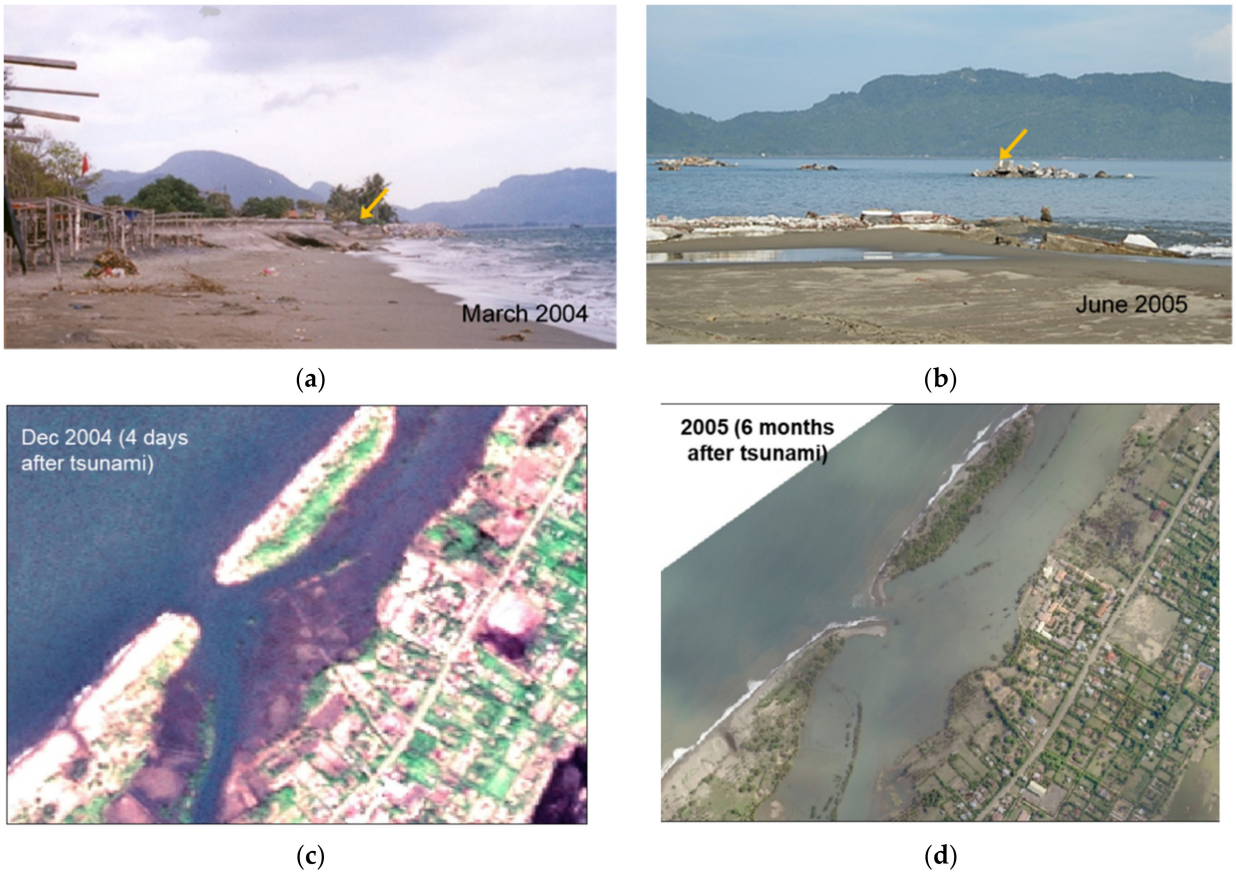

(**a**) (**b**)

(**c**) (**d**)

Figure 2. Indication of land subsidence at Lambadeuk, southwest of Banda Aceh coast: (**a**) The revetment located at the upper shoreface to protect the coast from further erosion nine months before the tsunami hit the coast on 26 December 2004; (**b**) The remnant of a seawall post-tsunami. The yellow arrows in both pictures show the same revetment; (**c**) The breaching of barrier island at Kuala Gigieng four days after the tsunami; (**d**) The development of sand spit growth six months after the tsunami, to reconnect the breached barrier islands at Kuala Gigieng.

At the northern Sumatra, the fault system splits into two active segments, i.e., Aceh Segment and Seulimum Segment (Figures 1b and 3a). Natawidjaja and Triyoso [28] found that currently, those segments possess a seismic gap of 325 km and 70 km long in the last 100 years, respectively, and considered them as an alarming hazard potential in the future. The highly populated Banda Aceh city is situated between these two segments (Figure 3a). The coast is facing the Andaman Sea and is semi-embayed by the entraining forearc small islands at the north off-shore from the rough, energetic waves of the Indian Ocean to the west. Lambadeuk exemplifies a relatively broad lowland coastal system overlying a major segment of the active tectonic fault, i.e., Aceh Segment. Kuala Gigieng displays a marine-dominated coastal system. The mainland consists of old parallel coastal ridges and swales. In the last few centuries and beyond, both coasts were naturally protected by the Late Holocene barrier islands as the coastal system's seaward-most land boundary. The alongshore multitemporal bathymetric profiles in Figure 3b illustrate the averagely shallow bathymetry in front of Kuala Gigieng, and the tilting southwest towards Lambadeuk, where considerably deep trenches are observed in two consecutive years in 1893 and 1924. In contrast, the bathymetry around the same location appears to have been remarkably shallow in 2006.

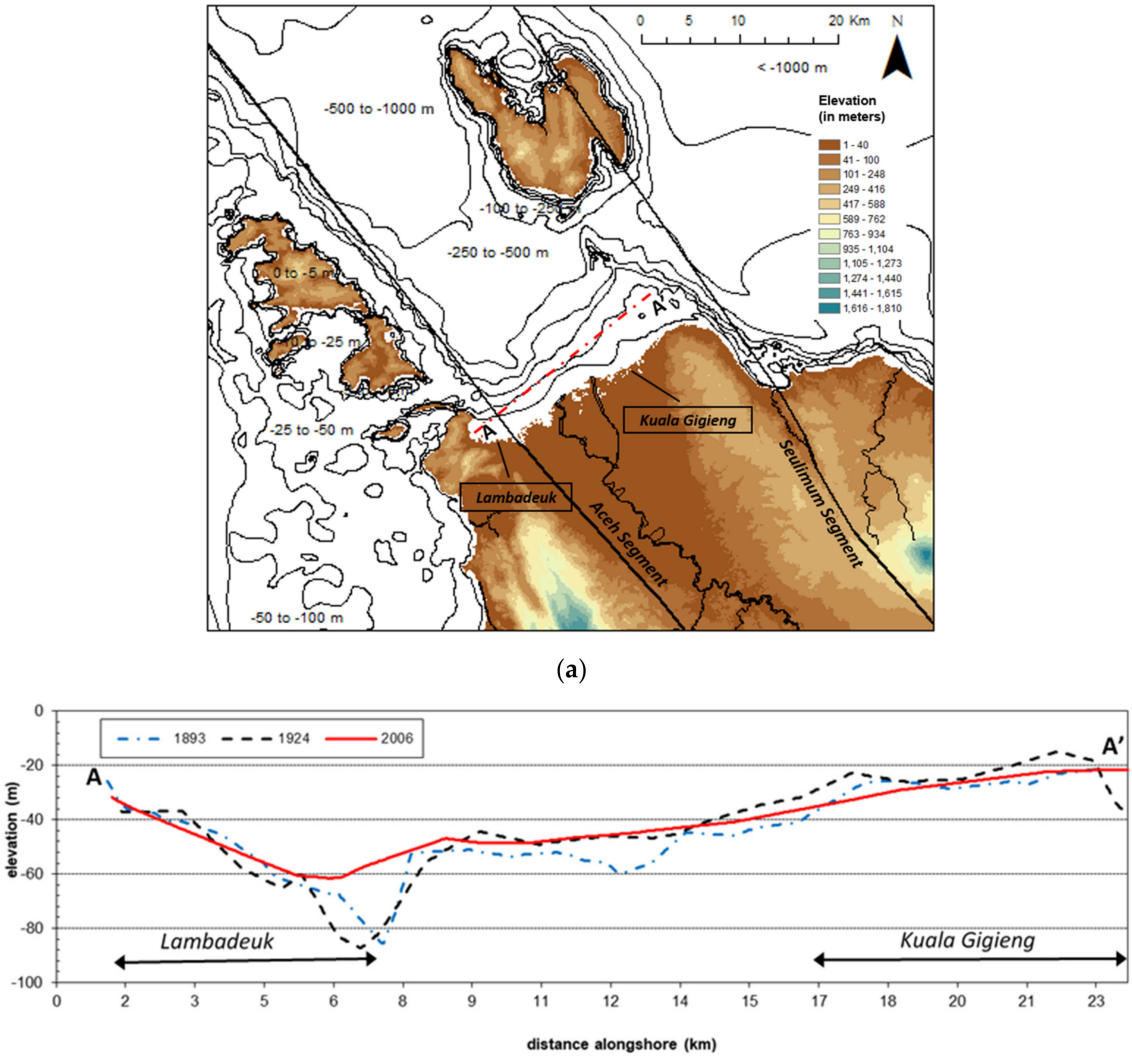

Figure 3. Banda Aceh is situated in the wedge between two tectonic fault segments of the Great Sumatran Fault System, i.e., the Aceh Segment on the southwest and Seulimum Segment on the northeast: (**a**) The map shows the topographic and bathymetric contours of the northern Sumatra region, and the two fault segments; (**b**) The multitemporal alongshore bathymetric profiles in front of Banda Aceh coast show higher elevation at Kuala Gigieng and lower down towards Lambadeuk. The bathymetric data of the year 1893 and 1924 was digitized from the Dutch Colonial Nautical Chart obtained from KITLV, and the 2006 bathymetry was obtained from the bathymetric survey conducted by UP-PSDA of Syiah Kuala University.

The tides along the coast are categorized into a micro-tidal regime which is on average less than one meter high. The typical equatorial monsoonal climate brings about seasonal prevailing wind-induced wave heights and periods variations, i.e., southwesterly during April to September and northeasterly during October to March [22]. The Aceh River is the primary natural river crossing the low-lying coastal city of Banda Aceh (Figure 1c). The river course has been artificially bifurcated at 10 km upstream to a 300 m wide artificial Alue Naga Floodway Canal since the early 1990s, another major outflow dissecting the coastline at present. Both major outlets are the primary sources of sediment supply to the coastal system of the investigated area. Currently, both are regulated by training jetties to maintain navigational depth for fishing boats. Another smaller river that flows at the northeast flank of Banda Aceh plain is the Angon River (Figure 1c), which has been non-

migratory throughout the last century, debouching into the shore-parallel lagoon behind the Kuala Gigieng inlet.

The coastal area was relatively densely populated prior to the 2004 tsunami event, occupied by approximately 250,000 people. Around half of the total population has been reported dead or gone missing [45] after the 2004 mega tsunami. More than a decade since the tsunami event, the coastal city has been rehabilitated and reconstructed. Despite the devastation due to the earthquake and tsunami, people are likely to return to their original living and business locations close to the coast. By 2009, the post-tsunami rehabilitation and reconstruction program in Banda Aceh had established resettlement at the coastal area up to 91% [46], along with all the necessary infrastructure such as a ferry port, religious and administrative buildings, schools, housing areas, and a sanitary landfill [23]. Apart from having been recovered from the tsunami event, the coastal area has been subjected to frequent flooding during high spring tides [47,48]. The coastal area is also vulnerable to hydrometeorological hazards, exceptionally high risk to the future sea-level rise [23]. We recently investigated the scenarios of coastal inundation due to the slow-onset projected sea-level rise in the next couple of centuries. The results show that the increasing number of built areas closer to the coastline, despite past tsunami experience, are potentially subject to tremendous loss due to seawater inundation in the next couple of centuries [23]. Such conditions provoke socio-economic and environmental vulnerability for the entire coastal area [49].

3. Materials and Methods

Historical records of particular events leading to morphological alteration are indispensable resources for better understanding the chronological implication to the state of coastal morphology. Previous studies have taken a similar approach by using the history of a few large-scale tectonic events to investigate the meso-term coastal changes (e.g., [50–52]). Herein, we consider that a multi-decadal timescale is appropriate to capture any remarkable changes in the coastal morphology induced by those extreme events associated with seismic activity, and also suitable for coastal management planning [53].

3.1. Spatial Data

We digitized shorelines from various data sources, i.e., from Colonial topographic maps of the 19th century and more recent satellite images of different spatial resolutions, the details of which are listed in Table 1.

Table 1. Spatial data sources for shoreline change detection.

Data Type	Date/Time	Spatial Scale/Resolution	Source
Topographic maps	1898 1924	1:20,000 1:50,000	KITLV
Satellite images	5 June 1967 23 March 1989 8 March 2000 30 June 2005	2.0 m pixel resolution 30 m pixel resolution 30 m pixel resolution 2.5 m pixel resolution	KeyHole-7/USGS Landsat TM/LAPAN Landsat ETM/LAPAN NORAD survey/SIM Centre–BRR NAD
	10 January 2017	1.5 m pixel resolution	IKONOS/LAPAN
Photogrammetric topographic map	June 2005	0.5 m contour interval	NORAD survey/JICA/SIM Centre–BRR NAD

All data sources were geo-referenced to a master map (i.e., ortho-rectified aerial photo acquired in June 2005 from the NORAD survey) processed in ArcGIS 10.6.1 to have a common horizontal datum, projection, and coordinate system. Figure 4 shows the samples of the multisource and multitemporal data used in this study.

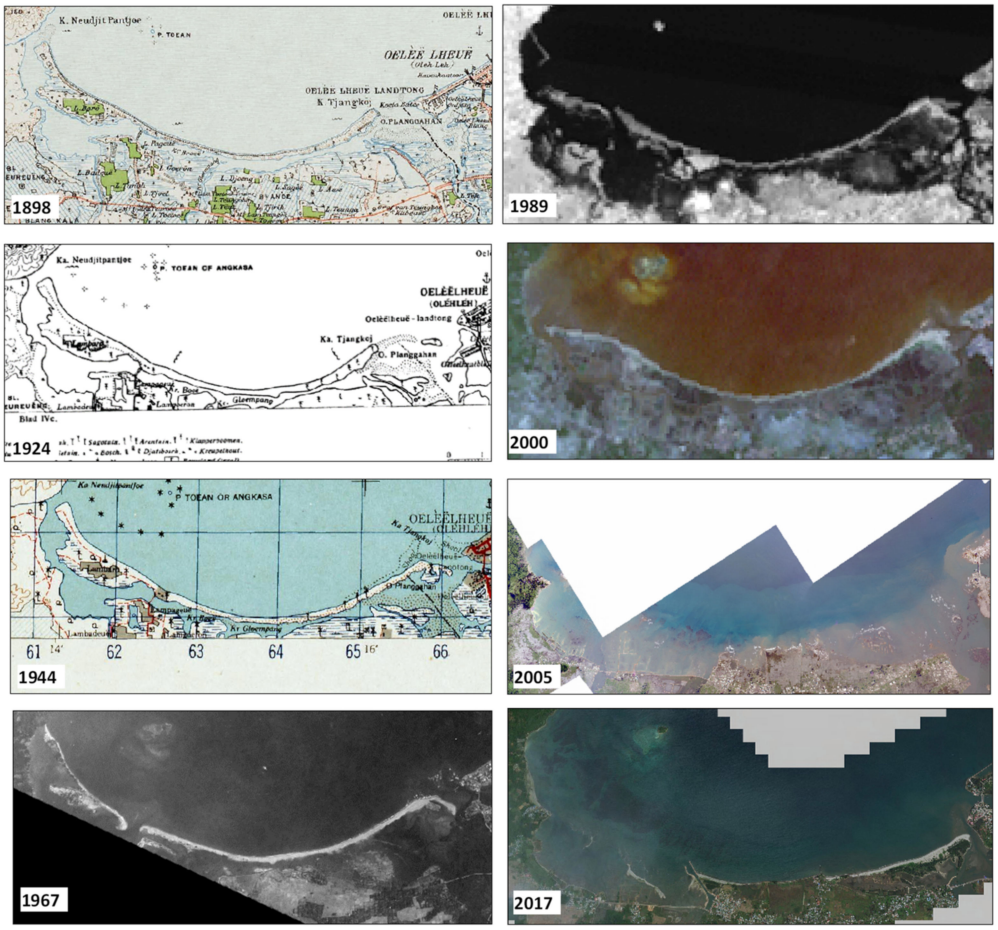

Figure 4. Samples of the multisource topographic maps and satellite images of the Lambadeuk coast, displaying a highly varying data type and quality. Information about the data details can be found in Table 1.

3.2. Historical Records of Earthquake and Tsunami Events

To support our spatial analysis using the historical maps and satellite images, we corroborate the records and results of studies of the earthquake events in the Indian Ocean/Andaman Sea region and along the northern part of the Great Sumatran Fault System. The underlying active fault system along the Sumatra Island is one of the most significant active faults in the world, with slip rates ranges from 10 to 27 mm/year [28]. Natawidjaja and Triyoso [28] identified that the Great Sumatran Fault has at least 19 segments along the fault zone. More than a dozen large earthquakes have occurred historically in the past two centuries associated with the fault zone. Similarly, Hurukawa et al. [43] concluded in their study that almost all the earthquakes occurred since 1892 at Sumatra Island were located at Sumatran Fault, with high seismic hazard mainly occurred over the entire northern part of Sumatra Island during the period of 1942–2003.

Here, we limit the area of earthquake influence by setting up a regional boundary within which we identify any major ($M \geq 7.0$) and moderate ($6.5 \leq M < 7.0$) earthquake events records, as depicted in Figure 5. The historical earthquake records are obtained primarily from the NGDC/WDS Global Historical Tsunami Database of the National Centers for Environmental Information (NCEI) database [54]. Additionally, records were also obtained from the Catalogue of Significant and Destructive Earthquakes 1821–2017 for the earthquakes associated with the Great Sumatran Fault [55]. From the database we found five remarkable earthquake events which occurred within our investigation period, which are enlisted in Table 2. The locations of the earthquake epicenters are depicted in Figure 5.

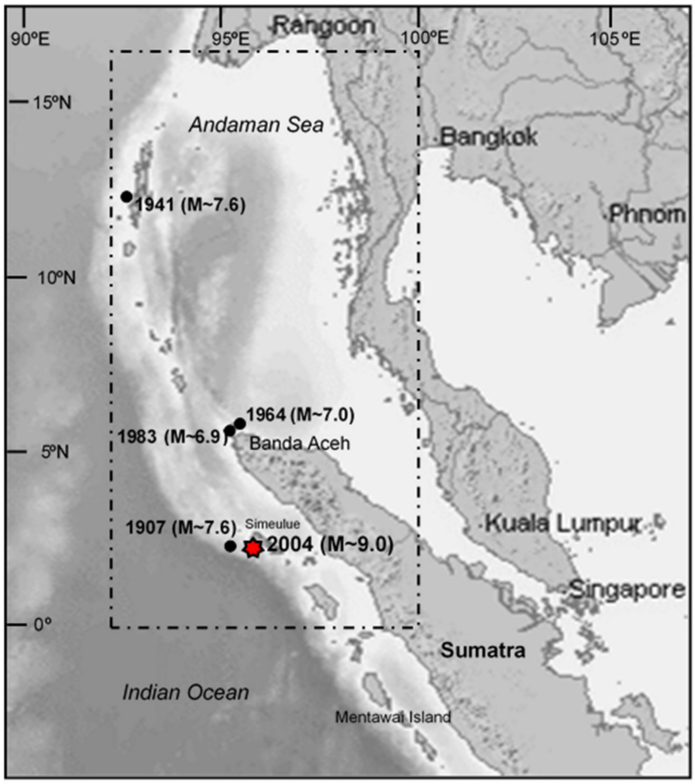

Figure 5. Regional earthquake occurrences at the northern Sumatra during the investigation period in the present study (1898–2017). The dashed-line rectangle shows the regional boundary of influence of the major ($M \geq 7.0$) and moderate ($6.5 \leq M < 7.0$) earthquake records. Records of earthquakes $M \geq 7.0$ accompanied with the validity of tsunami occurrences are retrieved from the earthquake catalog by [54], and the tectonic earthquakes associated with the Great Sumatran Fault obtained from [55].

Table 2. Earthquakes leading tsunami events affecting Banda Aceh in the period of 1804 to 2004. Geographical boundaries displayed in Figure 4.

Date	Latitude (° North)	Longitude (° East)	Focal Depth (km)	Location	EQ Magnitude	Tsunami Validity *
4 January 1907	2	94.5	50	NW Sumatra (Simeulue Island)	7.6	4
26 June 1941	12.5	92.5	20	Andaman Sea	7.6	4
02 April 1964	5.6	95.4	60	NW Sumatra	7.0	3
04 April 1983 **	5.7	94.7	78	NW Sumatra	6.9	No evidence
26 December 2004	3.3	96	30	Off West Sumatra	9.0	4

Note: * Data source from [54]; 4 = definite tsunami; 3 = probable tsunami; 2 = questionable tsunami; 1 = very doubtful tsunami; 0 = event like a seiche. ** Data source from [55].

The NCEI database is accompanied by the reports of the past earthquakes and their associated resulting hazards (e.g., tsunamis, earthquake damage, liquefaction, etc.) that were mostly archived by Soloviev and Go [56] and also by several other scientific documents and papers. Here, the tsunami event records were gathered from scientific and scholarly sources, regional and worldwide catalogs, tide gauge reports, individual event reports, and unpublished works. Descriptions of tsunami events with various occurrence validity levels associated with some earthquake records were used in this study to identify the number of possible tsunami events in the last couple of centuries [57,58]. The level of validity ranges from 1 (less probable occurrence) to 4 (most probable occurrence). It also specifies the tsunami events that occurred at specific locations from where any tsunami waves would have propagated towards their surrounding coastlines. A complete discussion of possible errors can be found in [57].

3.3. Storminess

There is merely a little overview of the climatic condition in the last century in the investigated area. Verstappen [7] reported that, in general, the climatic condition at the northern tip of Sumatra island was relatively dry in the last century. The equatorial position of Indonesia shelters it from tropical cyclones that often devastate the Philippines, Sri Lanka, Bangladesh, and the coastal zone of western Australia. The recent studies [59–61] of the historical cyclones over the Bay of Bengal and the Andaman Sea reveals that the pathways of the cyclones revolve around the latitudes of higher than 8° N. Accordingly, the coastal areas at the northern tip of Sumatra (5° N) are assumed to experience much weaker tropical storm events. Thus, remarkable breaching events of barrier islands, such as those identified in the present study, are unlikely as the results of tropical storms, which is particularly important to keep in mind when analyzing the possible forcing factors responsible for observable morphological changes in this study.

3.4. Regular Wave Climate and Littoral Transport Rate

We obtained the wave climate of the Banda Aceh coast by converting the eleven-year daily wind data records from 1995 to 2005 from the National Meteorology, Climatology and Geophysics Agency (BMKG), and subsequently translated into statistical wave heights and periods as functions of wind velocity, duration, and fetch. Surface and tidal currents are not well-recorded in this coastal region. The tides moderately range of 1.00 m from MHWL to MLWL. From the data, we found that the prevailing monsoonal wave directions were from the northwest and the northeast. Based on the resulting wave data, we then roughly estimate the littoral transport rate by using the simple CERC formula [62] at both Lambadeuk and Kuala Gigieng coasts. Estimates of net littoral transport along both coasts will be discussed in Section 4.

3.5. Analysis of Morphological Changes

Morphological changes of the seaward most barrier islands and spits in seven consecutive periods were analyzed in this study at the Lambadeuk and Kuala Gigieng coasts. Each period consists of shorelines of the seaward most barrier islands and spits of two consecutive years. Any changes found to be significant were measured as indicative figures to estimate the amount of displacement or growth of the morphological features.

4. Results

There is a substantial difference in geomorphic settings between Lambadeuk and Kuala Gigieng coasts. Lambadeuk, at the southwest flank of Banda Aceh city, is a transgressive coast built up during the Late Holocene. Typically, a transgressive Holocene coastal barrier underwent continuous erosion and roll-over so that the oldest washover stratigraphies are likely to have been erased [32]. On the other hand, the Kuala Gigieng coast at the northeastern flank is a regressive coast, which typically consists of coast-parallel ridges and swales environment. One can also observe consecutive ridge-swale morphology preservation at the highly energetic and marine-predominant coastal areas along the western coasts of Aceh, Sumatra, e.g., in [21,22].

Figure 6 displays the consecutive observation periods in this study, along with the identified earthquake events (or the absence of those) that occurred in each period. Each of the barrier islands and spits at the Lambadeuk and Kuala Gigieng have uniquely evolved and altered its shape, position, and vulnerability to seismic-related hazards impacts. The most significant changes are evident from a sequential comparison of the island and spit geometries and rates of areal changes. Figure 7a–j depicts the overall results of the delineation of both coasts' morphological features, covering the shorelines of barrier islands, sand spits, and the back-barrier intertidal areas. The sub-aerial parts of the morphological features are color-coded, and the sub-aqueous parts appear in white. Here, we display the shoreline delineations of 1898 and 2005 in every figure panels to provide references of the morphological states at the initial date and the date a few months after the 2004 tsunami

event. The latter is represented by the shorelines delineated from the high-resolution aerial photograph acquired in June 2005 (Table 1). In between those years, we then observe and analyze the successive pairs of barrier shoreline changes.

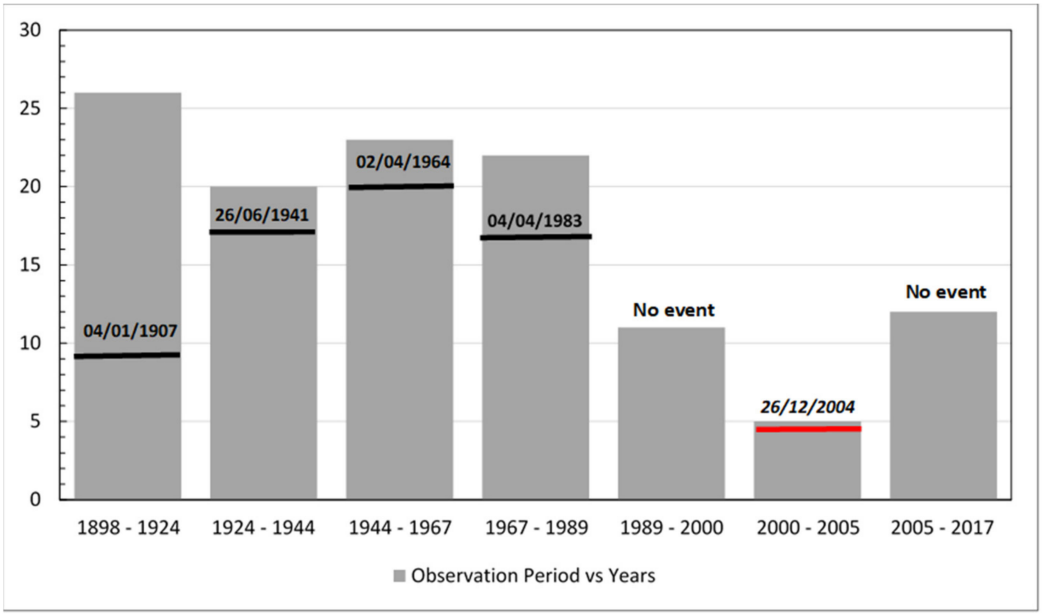

Figure 6. The observation of morphological changes of the northern tip coast of Sumatra Island, consists of seven periods with various intervals depending on the data sets available for comparison. The horizontal axis shows the consecutive periods of observation from 1898 until 2017, and the vertical axis is the length of each successive period of observation. Periods with remarkable earthquake events are marked by the bold black line indicating the year the event occurred, which shows how far away from the pair of observation years the event is. The horizontal red line in 2000–2005 indicates 26 December 2004, marking the earthquake that triggered the mega-tsunami.

We quantify the rate of change of the barrier islands' morphology by simply substituting the polygon areas of a pair of barriers' perimeters from two consecutive observation years, and dividing the result by the length of the period in between. To avoid misleading quantification of the rate of change, we exclude the quantification of the areal changes of the back-barrier lagoon and intertidal morphology. The misled quantification may come from sediment deposition to the back-barrier area from the barrier breaching and from the water inundation extend over the intertidal areas at the time the satellite image was acquired. Nevertheless, for the observation purposes, we still display the delineation of the morphological features at the back-barrier during each observation years, as was delineated from the datasets.

4.1. Rate of Change of Barrier Islands Morphology

From the wave data analysis, we obtained the seasonal prevailing monsoonal waves annually. The southwest monsoon occurs between April and September and is characterized by relatively rough waves coming from the northwest at the Banda Aceh coast. About 53% of the waves approach the coast with a significant wave height of 1.0 m with a period of 3 s. During the northeast monsoon between October and March, the climate tends to be milder, with 30% of the waves approaching from the northeast with a significant wave height of less than 1 m and a period of 4.5 s. Based on the resulting wave data, we then roughly estimate the littoral transport rate by using the simple CERC (CERC stands for Coastal Engineering Research Center, U.S. Army Engineer Waterways Experiment Station, Vicksburg, MS) formula [62], which results in the estimate of net littoral transports at a rate of +0.30 hectares/year and +1.08 hectares/year at Lambadeuk and Kuala Gigieng, respectively. The prevailing direction of net littoral sediment transport at both coasts is directed southwest, with positive rates suggesting the coasts are accretional.

Tables 3 and 4 display the rates of land gain or loss at Lambadeuk and Kuala Gigieng as the results of the barrier islands' morphological responses during the consecutive periods of observations. The largest amount of land loss is observed for all the barrier systems in 2000–2005 due to the impact of the 2004 earthquake and tsunami event, i.e., −73.54 hectare and −128.73 hectare at Lambadeuk and Kuala Gigieng, respectively. These are equivalent to a 100% and 59% loss of land with rates of −14.71 hectares/year and −25.75 hectares/year, respectively. Both rates are an order of magnitude higher than the estimate of the littoral transport rate under regular wave climate.

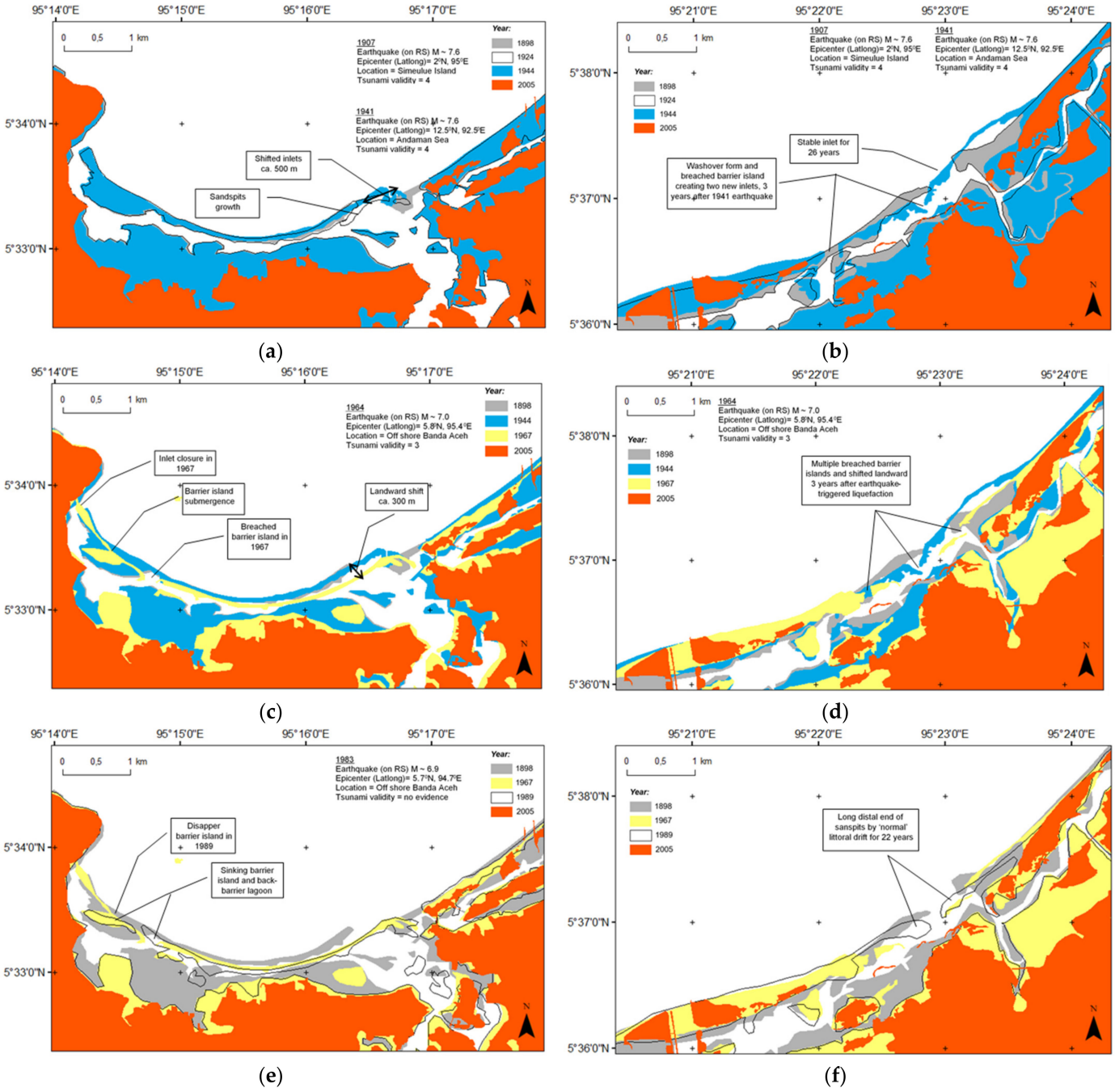

Figure 7. *Cont.*

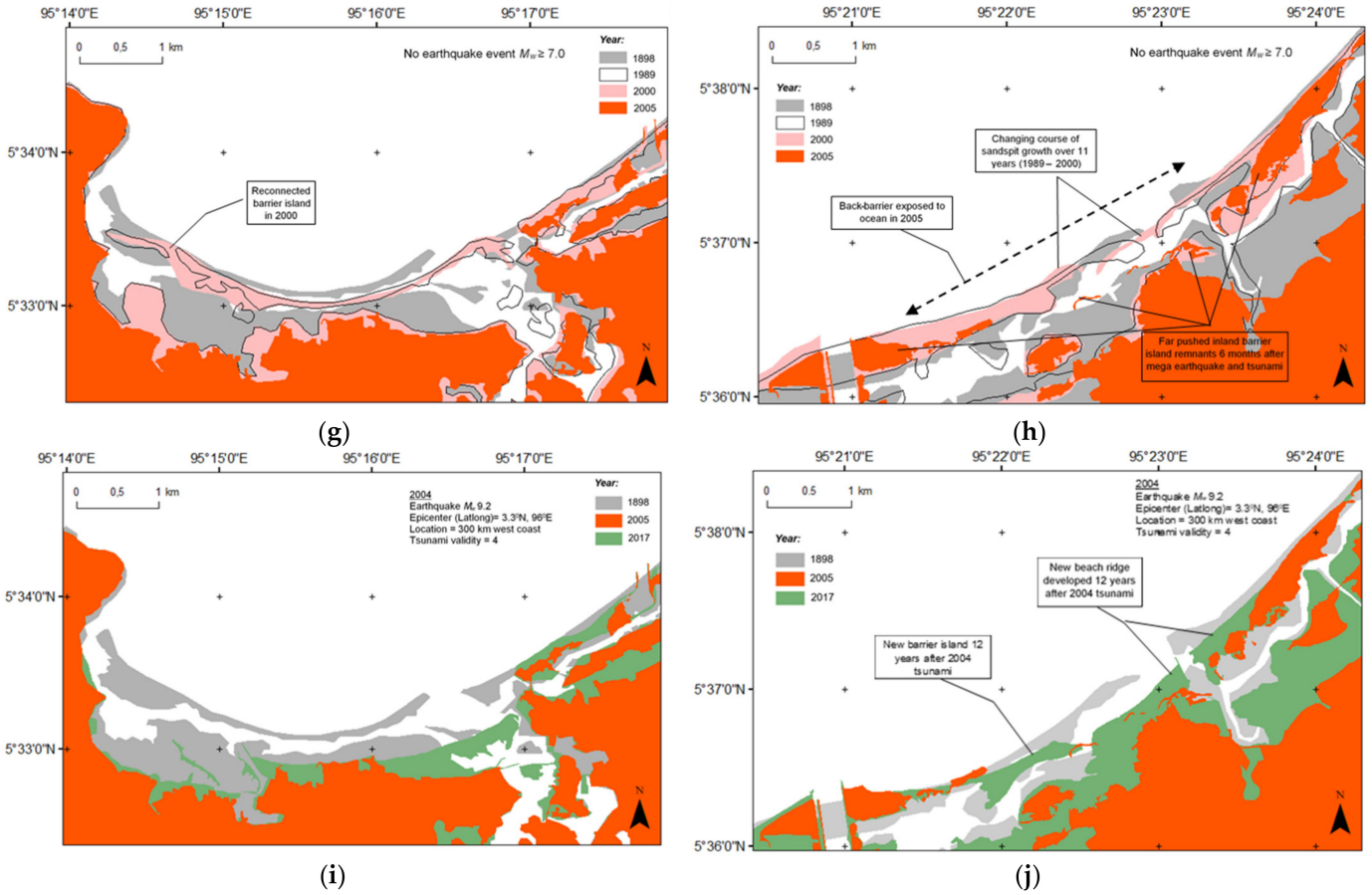

Figure 7. Observation of barrier island morphological changes from the consecutive pairs of shoreline delineation of Lambadeuk and Kuala Gigieng coastal section, at the northern tip of Sumatra Island: (**a**,**b**) Changes at Lambadeuk and Kuala Gigieng, respectively, in two periods 1898–1924 (26 years), and 1924–1944 (20 years). Major earthquakes occurred in both periods; i.e., on 4 January 1907 of *M* 7.6 which is most likely to have triggered a tsunami event (tsunami validity = 4), and on 26 June 1941, which triggered a far-field tsunami event; (**c**,**d**) Changes at Lambadeuk and Kuala Gigieng, respectively, in 1944–1967 (23 years), during which a major earthquake occurred on 2 April 1964, of which the epicenter was relatively close to Kuala Gigieng, and reportedly triggered tsunami and liquefaction; (**e**,**f**) Changes at Lambadeuk and Kuala Gigieng in 1967–1989 (22 years), during which a moderate earthquake occurred on 4 April 1983 of *M* 6.9, and the epicentre was just off-shore from the Lambadeuk coast. No reports on any tsunami event. However, Lambadeuk reportedly experienced tectonic land subsidence; (**g**,**h**) Between 1989 and 2000 (11 years), no significant earthquake occurred at both Lambadeuk and Kuala Gigieng; (**i**,**j**). Dramatic changes occurred in the period of 2000–2005. During this short period, the mega-tsunami triggered by one of the largest magnitude earthquakes to have occurred in the modern history occurred on 26 December 2004, of M~9.0.

Table 3. Average long-term historical rates of land area change for both coasts for selected periods at Lambadeuk. Rates are in hectares/year. Positive numbers indicate land gain, and negative numbers indicate a land loss.

Period	Length of Period (Years)	Areal Changes (Hectares)	Rates of Changes (Hectares/Year)	Percentage of Land Loss/Gain
1989–1924	26	+8.59	0.33	13%
1924–1944	20	+0.93	+0.05	1%
1944–1967	23	−31.79	−1.38	−41%
1967–1989	22	+9.69	+0.44	21%
1989–2000	11	+17.61	+1.60	31%
2000–2005	5	−73.54	−14.71	−100%
2005–2017	12	0.00	0.00	0%

Table 4. Average long-term historical rates of land area change for both coasts for selected periods at Kuala Gigieng coast. Rates are in hectares/year. Positive numbers indicate land gain and negative numbers indicate land loss.

Period	Length of Period (Years)	Areal Changes (Hectares)	Rates of Change (Hectares/Year)	Percentage of Land Loss/Gain
1989–1924	26	0.00	0.00	0%
1924–1944	20	−49.06	−2.45	−20%
1944–1967	23	−7.94	−0.35	−4%
1967–1989	22	+14.07	+0.64	8%
1989–2000	11	+21.30	+1.94	11%
2000–2005	5	−128.73	−25.75	−59%
2005–2017	12	+43.49	+3.62	49%

In the century before the mega-tsunami, Lambadeuk experienced significant land loss during 1944–1967 by −41%; nevertheless, it was compensated by 21% and 31% of land gain in the subsequent two consecutive periods (Table 3). Overall, Lambadeuk on average gained 5% extra land during the last century, only to face a complete loss of barrier island due to the 2004 tsunami until the present. In contrast, Lambadeuk experienced land loss of merely −1% averagely during the last century prior to the 2004 tsunami. The loss of barrier island area by −59% during the mega-tsunami has been compensated by 49% in 2017 since the tsunami.

4.2. Multitemporal Morphological Changes

The following is our analysis of the morphological changes of barrier islands and spits observable in Figure 7, and estimates of the total land loss or gain as the results of those changes based on the quantitative analysis described in Section 4.1. Following this analysis, the interpretation of possible controlling factors for those changes will be discussed in Section 5.

4.2.1. Period 1898–1924–1944

In these consecutive periods, the main barrier island at Lambadeuk is in a relatively stable position in 1898–1924 and 1924–1944 (Figure 7a). Despite a major earthquake occurring in 1907, the barrier islands at Lambadeuk and Kuala Gigieng show a relatively stable state of morphology, which is observable by comparing the shorelines of 1898 and 1924 (Figure 7a,b). The growth of barrier spits extended from the eastern end of the barrier island at Lambadeuk suggests no extreme forcing, which could have caused remarkable changes in the barrier's morphology, such as landward migrating or breaching. A relatively remarkable barrier breaching occurred, however, at the adjacent coastal section at Ulee Lheue (the eastern barrier island next to Lambadeuk in Figure 7a). The possible cause is inconclusive in this study, as there was no report of any tsunami or land subsidence occurred as a result of the major earthquake, at the investigated area; despite a well-known tsunami event which was reported at Simeulue Island at the southwestern offshore of Sumatra.

In 1924–1944, a barrier spit was growing further east as far as ca. 500 m, and almost connected to the remnant of a major breach of the Ulee Lheue barrier island (Figure 7a). In 1944, the spit was modified, along with slightly narrowing and counterclockwise re-orientation of the barrier island's eastern part. Meanwhile, at Kuala Gigieng, the barrier islands (appear in blue in Figure 7b) had undergone significant changes. Two new inlets were created while the entire sub-aerial part of the barrier island has shifted landward at a maximum distance of ca. 300 m at the central part, and the section at the northeast at the same time moved seaward at more or less the same distance. Furthermore, this new barrier island formation seems to be narrowing entirely, resulting in a total land loss of −49.06 hectares with an average rate of about −2.45 hectares/year (Table 4).

4.2.2. Period 1944–1967

In 1944–1967, the barrier islands and spits of both investigated coasts were significantly changing compared to the previous period. In 1967, both coasts experienced a relatively far landward shift, i.e., around 300 m distance, while the narrowing subaerial parts of the barrier features are remarkable (Figure 7c,d). Additionally, the barrier spits were breached at multiple locations at Kuala Gigieng (Figure 7d). A tectonic earthquake associated with the Seulimum segment activation occurred in 1964 with a magnitude M 6.7 [28,43], of which the epicenter was merely 73 km northeastern off-shore of Kuala Giging coast (Figure 5). The remarkable features of narrowing and breached barrier islands and spits remain observable in 1967, i.e., in merely three years after the earthquake event.

4.2.3. Period 1967–1989

In 1967–1989, most of the barrier islands and spits on both coasts became relatively stable, i.e., no barrier island migration was found. Nevertheless, the westernmost part of the barrier at Lambadeuk that appeared in 1944 disappeared in 1967 (Figure 7e), suggesting submergence of the barrier island. In contrast, at Kuala Gigieng, the barrier islands were in a stable position throughout the whole period (Figure 7f). It is noteworthy that in this period, there was a moderate earthquake of magnitude M 6.9 which occurred in 1983, of which the epicenter was located just off-shore from Lambadeuk (Figure 5 and Table 2), suggesting that the earthquake was associated with the Aceh Segment which was underlying the coast.

4.2.4. Period 1989–2000

There were no major or moderate earthquakes recorded in 1989–2000 (Table 2 and Figure 5). At Lambadeuk, the barrier island maintained its position during the 11 years, showing a stable and mature barrier spits at the eastern end. The previously submerged and breached barrier island in 1989 at the western end has been reconnected since (Figure 7g). At Kuala Gigieng, elongated barrier spits were developed, interestingly, in the opposite direction from the development that occurred during the last period. Although the barrier islands and spits position show no significant migration, a narrowing land area is apparent. The further growth of the right-hand barrier spit to the southeast appeared in 2000 (appeared in pink in Figure 7h) extending further southeast as far as 700 m from the tip of barrier spit in 1989.

4.2.5. Period 2000–2005–2017

The years between 2000 and 2005 were the remarkable period where the great earthquake triggering the mega-tsunami occurred and severely destroyed the northern tip coast of Sumatra Island on 26 December 2004. The change of morphological features along the coast was expectedly enormous. Figure 7i,j display the massive overwash of the entire investigated coast leading to several breaches, and the remnants of the barrier islands were shifted landwards. The stabilized barrier spit which appeared in 2000 had disappeared entirely (Figure 7i,j).

Twelve years after the 2004 tsunami, the shoreline in 2017 reveals a striking difference in both of the investigated coasts in responding to the tsunami waves. At Lambadeuk, after the disappearance of the entire barrier island (Figure 7i), the shoreline started to develop from the former lagoon's inner shore, which has since been exposed to the sea. Kuala Gigieng now has two relatively permanently open inlets because of the barrier island and barrier spit breaching during the 2004 tsunami (Figure 7j).

5. Discussion

Our investigation on the morphological changes of barrier islands and spits at two coastal settings along the northern tip of Sumatra Island revealed several new findings on the possible controlling factors associated with the seismic activity that change barrier island morphology. The intervals between periods of observation of morphological

changes are of less than 30 years, which fits the return period of major earthquakes in the region of Sumatra. The impact on the coastal morphology can be in the form of barriers breaching, sinking, landward migrating, and landward bending of spits development. The possible interplaying forcing factors to those morphological changes are discussed in the following subsections.

5.1. Tsunami Overwash

In 1944, the barrier island at Lambadeuk remained stable compared to its morphological state in 1924, with the additional growth of barrier spit (Figure 7a). In contrast, the barrier islands at Kuala Gigieng experienced a landward migration, breaching, and the growth of barrier spit bending landwards (Figure 7b). Such morphological pattern is typical for barrier islands washed over by storm events or hurricanes, e.g., Hurricane Sandy and Hurricane Katrina [40]. Energy dissipation is then mostly achieved through the overwash bore running over the barrier, flattening the barrier crest profile, and depositing off-shore originating material over the back-barrier zone [32]. Provided that the height of the barrier island was typically less than 2 m high [7], the forcing factor which possibly controls such morphological impact is a wave coming from the sea. Waves equal to or slightly higher than the height of a barrier island, with a fairly long period, may have overtopped some of the lowest points of the barrier island. Analogously to a storm event, among the four regime types of impacts caused by storm waves on a barrier island [32], the observable morphological changes at Kuala Gigieng in 1944 may fall into the "Overwash regime".

In 1924–1944, there were no earthquake events associated with either the Sunda Trench and the Great Sumatran Fault system that occurred near the northern tip of Sumatra Island in this period. However, a major earthquake of M 7.6 occurred in 1941 at the western coast of Car Nicobar Island, with its epicenter at 12.1° N and 92.5° E, or around 834 km northwest from Banda Aceh (see location in Figure 5). NCEI [54] recorded a high score validity tsunami event associated with this earthquake (Table 2). From the historical reports [63,64], the earthquake generated a tsunami throughout the Andaman Sea and the Indian Ocean. Despite the lack of reliable records, for instance from the tidal gauge, which was in operation at the time, some local newspapers in India reported that a tsunami was witnessed along the eastern coast of India. At the Nicobar and Andaman Islands, the wave heights were reported as high as 0.75–1.75 m. It was estimated that 3000 to 5000 people were killed in Sri Lanka and on the east coast of India [65]. Local newspapers believed to have mistaken the reported deaths and damage to a storm surge.

In support of these reports, a numerical model developed by [66] was to simulate the Andaman–Sumatra tsunami propagation of tsunami triggered by the earthquake that occurred in 1941. The result reveals an agreement with the documented observation reports that the earthquake felt over a wide area covering the eastern and southern Andaman Sea region (i.e., the northern coast of Sumatra). The model results show that the tsunami has reached the coast of Nagapittinam on the west coast of India after 165 min, with run-up heights in the range of 0.95–1.25 m, and the north tip of Sumatra at 120 with tsunami wave height was less than 1.00 m [66].

It is noteworthy to mention that following the earthquake, two events with magnitude 6.0 struck within 24 h after the main shock of 27 June 1941, and there were 14 aftershocks of magnitude up to 6.0 until January 1942 [67]. At Lambadeuk coast, McKinnon [68] reported that a local informant indicated that the location of the village of Lambaro, located at the western end of the barrier island of Lambadeuk (Figure 7a), had been moved three times within living memory, the last time being early in the Japanese occupation (1941–1942) when the inhabitants were forcibly removed from the shoreline and resettled at the foot of the surrounding hills. Thus, the far-field tsunami event in 1941 was most likely responsible for changes of the barrier islands and spits at Kuala Gigieng in 1924–1944. The nearshore bathymetry may have been controlling the tsunami arrival at the shoreline of Lambadeuk and Kuala Gigieng. The deepening bathymetry (Figure 3b) may help to dampen the

incoming tsunami wave energy at Lambadeuk, while the shallow bathymetry at Kuala Gigieng may have amplified the tsunami wave force.

5.2. Combined Liquefaction and Tsunami Overwash

The observation period of 1944–1967 exemplifies the period where the impact of both liquefaction and tsunami occurred, and the effects are observable on both coasts. The barrier islands and spits delineated from the satellite image in 1967 in Figure 7c,d show the state of the coast three years after a major earthquake event on 2 April 1964 of magnitude *M* 7.0, which epicenter located at 5.6° N and 95.4° E (see Table 2), or ca. 12 km northeastern off-shore of Banda Aceh City. The barrier islands and spits at both coasts experienced hundreds of meters of landward migration (and slightly reoriented clockwise at Lambadeuk), multiple-barrier breaching, especially at Kuala Gigieng coast, as well as a narrowing of subaerial parts of barriers, most probably as a result of land subsidence induced by liquefaction (Figure 7b,c). Surprisingly, the multiple inlets as the results of breaching events remained open even after three years of development, suggesting that littoral transport and sediment supply under the regular wave climate have not made up for the loss of land caused by the tsunami and liquefaction.

Soloviev [56] reported that an earthquake that occurred on 2 April 1964 had caused considerable damage to adobe buildings, the ground cracked open, the ground subsided, mud and sand gryphon appeared. Such impacts of ground shaking are comparable to our observation on the 2016 Pidie Jaya tectonic fault earthquake of *M* 6.5, in Pidie Jaya district on the northern coast of Aceh Province [69]. In Pidie Jaya earthquake, black sandy mud emerged through small cracks opening in the internal floors of houses. Both coasts are comparable for their similar type of wave-dominated sandy coastal area with typical soil type of alluvium containing gravels, sands, and muds [70]. Such soil structure provides some degree of tremor amplification [69], which creates saturation on sandy layers and increases pore water pressure, leading to liquefaction [71].

NCEI [54] recorded a high-validity event of the tsunami (validity 3), mostly based on a report by [56], in which a combination of a tidal (tsunami) wave and the locals observed land subsidence of half a meter at Ulee Lheue, east of Lambadeuk barrier island (Figure 7c). The multiple breachings that appeared at Kuala Gigieng in 1967 (Figure 7d) may have been further submerged by the already breached barrier islands in the earlier period (1924–1944), suggesting an effect of liquefaction combined with a tsunami overwash.

5.3. Co-Seismic Tectonic Subsidence

The observation period of 1967–1989 reveals a unique contrasting development of barrier system morphology between the two observed coasts. Contrary to the long-distance growth of sand spits to their distal length observed at Kuala Gigieng (Figure 7f), the western side of barrier island at Lambadeuk (Figure 7e) appeared to have been heavily subsided, that the slightly more than 1 km barrier island connected to the Ujong Pancu headland which appeared in 1967 and had disappeared entirely in the satellite image of 1989. This left a piece of subaerial part detached from the main barrier island. Such contrasting changes most likely have something to do with tectonic activities within the period.

A moderate tectonic earthquake occurred on 4 April 1983 with magnitude *M* 6.9 [72], and the epicenter was located at 70 km northwest off-shore of Banda Aceh (Figure 5, Table 2). The earthquake caused significant damage to buildings in Banda Aceh city, with the Mercalli scale recorded as category VI [55]. There was no report from the locals of any tsunami occurrence or liquefactions such as those which occurred in 1964. It is also noteworthy that the submerged area is close to the underlying Aceh Segment, suggesting tectonic subsidence responsible for the submergence. McKinnon [73] investigated the archaeological artifacts at this location, which suggests localized tectonic subsidence in the vicinity of the Sumatran Fault System, which appeared to be dramatically evident around Lambadeuk. Strong evidence of submergence came from the rectangular structure discernible during the low tides, which happened to be a former mosque foundation that

remained visible underneath the water in an aerial photograph from 1978. An interview with a local informant suggested that in the last 80 years towards the first Japanese occupation in 1942, a sunk off the coast at least two to three meters had been occurring [73]. The shoreline had retreated about 150–200 m at a village called Lambaro, which was originally located at the Lambadeuk barrier island. This village, which had already been moved three times, was eventually rebuilt about 12 km inland at present. Bearing in mind that this area has evidently been submerged in two consecutive periods, i.e., 1944–1967 and 1967–1989, this suggests that Lambadeuk is not resilient to multiple tectonic subsidence.

5.4. Dormant Period of Major and Moderate Earthquake

Among the entire periods of our investigation, there was also a period where major or moderate earthquakes were absent, which was during 1989–2000 (Figure 7g,h). Based on the work of Nott et al. [33], one might have expected that less intense storm periods would have induced a slowing down of the development of beach ridges (in this case, the barrier islands). Instead, we note that the reconnection of the previously breached barrier islands occurred during this period (Figure 7g,h). Moreover, the further growth of the barrier spit at Kuala Gigieng towards the opposite direction from the previous period (Figure 7h) suggests that the prolonged net littoral drift prevailing southwestern direction is most likely responsible for the observed changing course spit growth.

Despite the stable development of barrier islands morphology during the non-event periods by the littoral process, the development of barrier islands depends on the continuous sediment supply from the rivers. A consistent prevailing longshore drift can promote such stable elongated barrier spit growth in a considerably long period, without any remarkable disruption such as by tectonic events [74]. A continuous sediment supply from the major outlets may have facilitated the growth of long barrier spits to their distal lengths, whereas the seasonal change of littoral drift between the alternating rough west monsoon and calm northeast monsoon may promote the spits' balanced growth.

5.5. Mega Tsunami Overwash

The great earthquake of 26 December 2004 has generated not only a tsunami but also land subsidence along the northern tip coast of Sumatra, particularly along its western coast. There were only a few meters of land subsidence that occurred in Banda Aceh [16,18]. The locals also observed liquefaction effects of clayed soils in many areas at Banda Aceh city [8]. Despite these, the far-field gigantic tsunami waves of more than 10 meters in height arrived at the northern tip of Sumatra and were most definitely the controlling factors of the remarkable changes of the barrier islands at Lambadeuk and Kuala Gigieng. This includes the extensive disappearance of the barrier islands (Figure 7i,j), which had long been preserved as the natural coastal protection to the back-barrier ecosystem since the Late Holocene.

Even after 14 years of post-tsunami develpment, the coastal area remains exposed to the ocean with the absence of a new barrier island. Clearly, the 2004 tsunami event has been the primary forcing factor responsible for the disappearance of most parts of the barrier islands at Lambadeuk and Kuala Gigieng (Figure 7g,h). For the case of a tsunami, out of the four types of storm regimes and prediction of beach changes proposed by [35], the presumable tsunami overwash that occurred in the 2004 event most probably falls into regime 4: "Inundation regime". Here, the barrier islands were overtopped by the tsunami, of which the height is considerably higher than the crest of the barrier island, overtopping the barrier island and flattening the barrier topography.

5.6. Fluvial and Lagoon Systems

The three major outlets supplying sediments to the coastal area are the Aceh River, Alue Naga Floodway Canal, and Angon River. All of them have been generally stable in their position throughout the entire investigated period, even after the 2004 tsunami. Small river streams flowing into the lagoon system have not been migrating from their original

position during the period of investigation, particularly those the locations of which were not directly associated with the tectonic fault (e.g., Sumatran Fault) and the length of the river streams are relatively short, i.e., less than 2 km. Combined with wave actions, in particular at the wave-dominated Kuala Gigieng coastal system, the sediment supply may have been actively contributed to the relatively quick reconnection of the barrier island breaching and the overall recovery of the associated barrier islands.

Verstappen [7] characterized the Sumatran river system, whereby the river discharge was affected by the monsoon. The sand fraction of the material carried off by the rivers and reaching the sea usually is considerably small as a result of the intense chemical weathering inherent in the prevailing humid tropical environment. Moreover, in the locations where neo-tectonism is dominant, the prevailing climatic conditions are less important compared to those at the more seismically stable locations.

5.7. The Morphological Resilience of Tectonically-Active Coasts

The present study reveals that major and moderate earthquakes with a return period of 20 to 30 years at the north tip of Sumatra Island of Indonesia have the potential to trigger tsunamis and co-seismic land subsidence and liquefaction. Figure 8 summarizes the varying land areas of barrier islands from one period to another subject to the presence of major or moderate earthquakes or the absence of them at Lambadeuk and Kuala Gigieng. In the previous discussions, we have been able to identify several different cases of morphological changes of barrier islands, which were driven by various controlling factors associated with major and moderate earthquake events in the last century.

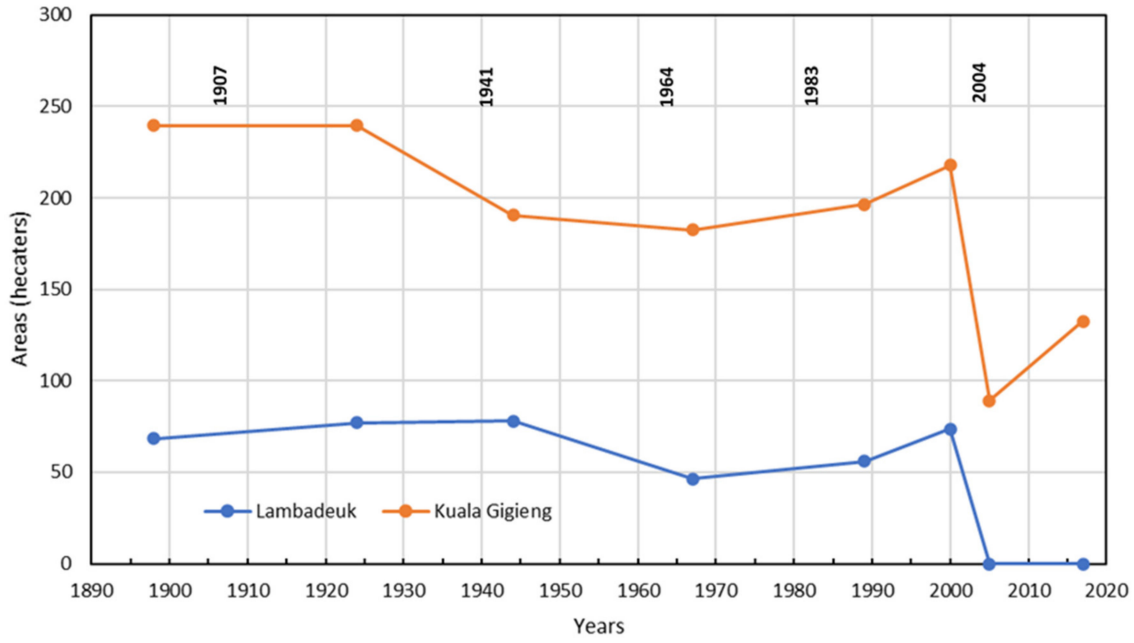

Figure 8. Historical land area trends for the Lambadeuk and Kuala Gigieng barrier islands to the timing of major earthquakes that impacted the islands.

The mega-tsunami of 2004 remarks the fundamental changes in terms of coastal morphological characteristics, i.e., from a low-lying wetland ecosystem naturally protected by barrier islands and spits into a wave-exposed intertidal coastal area. The sediment transport under the present day's wave regime is unlikely capable of restoring the removal of those barrier islands that was built during the Late Holocene, most probably under an extremely different wave regime. Thus, we may conclude that both Lambadeuk and Kuala Gigieng are not resilient to a mega-tsunami.

For the case of barrier islands directly associated with the tectonic fault system, a combination of co-seismic subsidence, liquefaction, and tsunami can dramatically change

the barrier island morphology, such as Lambadeuk. As for barrier islands located away from the tectonic fault system, such as Kuala Gigieng, the tsunami and liquefaction are responsible for modifying the barrier morphology, either independently or simultaneously. The breaching, landward migration, and the sinking barrier islands which occurred in the consecutive periods have been proven irreversible, despite a temporary growth of extended barrier spits at a sediment-rich environment. The unrecovered breaching, the submergence, as well as the disappearance of barriers observed even before the event of mega-tsunami of 2004, suggest that the barrier islands are not resilient enough against the recurrence of seismic events.

Evidently, within a century, the recurrence of several major earthquakes, either associated with subduction or tectonic fault zones, may trigger secondary effects, which potentially reduce the functionality of barrier islands and spits as natural coastal protection. The recurrence of small tsunamis, tectonic land subsidence, and liquefaction falls within an engineering timescale, which, therefore, should ultimately be taken into account in managing such a tectonically active coastal settings.

6. Conclusions

The present study investigates the resilience of barrier islands and spits because they protect low-lying coastal areas with high economic and environmental value. This is particularly true in archipelagic countries like Indonesia. Spatial analysis of barrier islands and spits is delineated in GIS, utilizing a multitemporal and multisource data series from the old Colonial topographic maps to the most recent high-resolution satellite images of 1898 to 2017, which encompasses a multidecade timescale observation. The earthquake and tsunami records and established conceptual models of storm effects to barrier systems are corroborated to support possible forcing factor interpretations. We found that tsunami, co-seismic subsidence, and liquefaction are the secondary effects of moderate or major earthquake occurrences that mostly control the state of the modern barrier islands and spits morphology in the investigated coastal area. Those controlling factors intermittently disrupt and interplay with sediment transport otherwise induced by regular wave climate, and eventually alter the coastal morphology development trend in the long term. The records of earthquake occurrences in front of the Banda Aceh coast suggest a return period of 20 to 30 years of major and moderate earthquakes, most of which triggered tsunami events (e.g., earthquakes in 1907, 1941, and 1964), and have far weaker wave energy than the one that occurred in December 2004. Evidently, liquefaction and co-seismic subsidence are the other controlling factors contributing to the remarkable morphological changes, which in some cases may be coupled with tsunami events. The results demonstrate that the semi-protected embayed Lambadeuk coast has been progressively lost its barrier islands due to repeated co-seismic subsidence. The wave-dominated Kuala Gigieng coast is not resilient to the combination of tsunami and liquefaction events. The mega-tsunami triggered by the 2004 earthquake has led to irreversible changes in both coasts' barrier systems. The barrier system is supposed to be a natural protection measure for the ecosystem and the economic value of the protected back-barrier domain. The exposed coastal mainland due to the barrier system disappearance may increase the risk of disaster by tsunamis, co-seismic subsidence, and liquefaction in the future. A further comprehensive evaluation of the resilience of the tectonically active coast, therefore, needs to be done. For such a dynamic tectonically active coastal area, investment in coastal protection to protect the invaluable ecosystem, and economic activities on the back-barrier domain will, therefore, be challenging. The results of the present study imply that in managing the coastal area where seismicity is highly active, despite small magnitudes, tsunamis, liquefaction, and land subsidence should be considered well.

Author Contributions: Conceptualization, E.M., F.L. and B.P.; methodology, E.M., F.L., M.D.-J.; software, E.M., F.L.; validation, E.M., F.L., P.W.; formal analysis, E.M.; investigation, E.M., P.W.; resources, E.M., D.D.; data curation, E.M.; writing—original draft preparation, E.M.; writing—review and editing, B.P., F.L., M.D.-J.; visualization, E.M.; supervision, M.D.-J., F.L.; project administration,

D.D.; funding acquisition, E.M., D.D. All authors have read and agreed to the published version of the manuscript.

Funding: This research was funded by the Indonesian Ministry of Research, Technology and Higher Education (Ristekdikti) through Scheme for Academic Mobility and Exchange (SAME) Program and World Class Professor Program (WCP) Scheme A.

Institutional Review Board Statement: Not applicable.

Informed Consent Statement: Not applicable.

Data Availability Statement: The data presented in this study are available on request from the corresponding author.

Conflicts of Interest: The authors declare no conflict of interest.

References

1. Daniell, J.E.; Schaefer, A.M.; Wenzel, F. Losses Associated with Secondary Effects in Earthquakes. *Front. Built Environ.* **2017**, *3*, 30. [CrossRef]
2. Bradley, K.; Mallick, R.; Andikagumi, H.; Hubbard, J.; Meilianda, E.; Switzer, A.D.; Du, N.; Brocard, G.; Alfian, D.; Benazir, B.; et al. Earthquake-triggered 2018 Palu Valley landslides enabled by wet rice cultivation. *Nat. Geosci.* **2019**, *12*, 935–939. [CrossRef]
3. Sunamura, T. *Geomorphology of Rocky Coasts*; Wiley: Chichester, UK, 1992.
4. Bird, E.C.F. *Coastal Geomorphology: An Introduction*, 2nd ed.; John Wiley & Sons: West Sussex, UK, 2011.
5. Stutz, M.L.; Pilkey, O.H. Open-Ocean Barrier Islands: Global Influence of Climatic, Oceanographic, and Depositional Settings. *J. Coast. Res.* **2011**, *272*, 207–222. [CrossRef]
6. Sui, L.; Wang, J.; Yang, X.; Wang, Z. Spatial-Temporal Characteristics of Coastline Changes in Indonesia from 1990 to 2018. *Sustainability* **2020**, *12*, 3242. [CrossRef]
7. Verstappen, H.T. *Outline of the Geomorphology of Indonesia: A Case Study on Tropical Geomorphology of a Tectogene Region*; ITC Publication: Enschede, The Netherlands, 2000; Volume 79.
8. Lavigne, F.; Paris, R.; Grancher, D.; Wassmer, P.; Brunstein, D.; Vautier, F.; Leone, F.; Flohic, F.; De Coster, B.; Gunawan, T.; et al. Reconstruction of tsunami inland propagation on December 26, 2004 in Banda Aceh, Indonesia, through field investigations. *Pure Appl. Geophys.* **2009**, *166*, 259–281. [CrossRef]
9. Narayana, A.C.; Tatavarti, R.; Shinu, N.; Subeer, A. Tsunami of December 26, 2004 on the southwest coast of India: Post-tsunami geomorphic and sediment characteristics. *Mar. Geol.* **2007**, *242*, 155–168. [CrossRef]
10. Paris, R.; Lavigne, F.; Wassmer, P.; Sartohadi, J. Coastal sedimentation associated with the December 26, 2004 tsunami in Lhok Nga, west Banda Aceh (Sumatra, Indonesia). *Mar. Geol.* **2007**, *238*, 93–106. [CrossRef]
11. Paris, R.; Wassmer, P.; Sartohadi, J.; Lavigne, F.; Barthomeuf, B.; Desgages, E.; Grancher, D.; Baumert, P.; Vautier, F.; Brunstein, D.; et al. Tsunamis as geomorphic crises: Lessons from the December 26, 2004 tsunami in Lhok Nga, West Banda Aceh (Sumatra, Indonesia). *Geomorphology* **2009**, *104*, 59–72. [CrossRef]
12. Umitsu, M.; Tanavud, C.; Patanakanog, B. Effects of landforms on tsunami flow in the plains of Banda Aceh, Indonesia, and Nam Khem, Thailand. *Mar. Geol.* **2007**, *242*, 141–153. [CrossRef]
13. Meilianda, E.; Dohmen-Janssen, C.M.; Maathuis, B.H.P.; Hulscher, S.J.M.H.; Mulder, J. Short-term morphological responses and developments of Banda Aceh coast, Sumatra Island, Indonesia after the tsunami on 26 December 2004. *Mar. Geol.* **2010**, *275*, 96–109. [CrossRef]
14. Yunus, A.P.; Shahabi, H.; Avtar, R.; Narayana, A.C. Shoreline and Coastal Morphological Changes Induced by the 2004 Indian Ocean Tsunami in the Katchal Island, Andaman and Nicobar—A Study Using Archived Satellite Images. In *Coastal World Heritage Sites*; Dou, J., Yunus, A.P., Santiago-Fandino, V., Eds.; Springer: Cham, Switzerland, 2016; Volume 14, pp. 65–77.
15. Wong, P.P. Rethinking post-tsunami integrated coastal management for Asia-Pacific. *Ocean. Coast. Manag.* **2009**, *52*, 405–410. [CrossRef]
16. Gibbons, H.; Gelfenbaum, G. Astonishing wave heights among the findings of an international tsunami survey team on Sumatra. In *Sound Waves*; USGS: Reston, VA, USA, 2005.
17. Borrero, J.C. Field survey of northern Sumatra and Banda Aceh, Indonesia after the tsunami and earthquake of 26th December 2004. *Seismol. Res. Lett.* **2005**, *76*, 312–320. [CrossRef]
18. Meltzner, A.J.; Sieh, K.; Abrams, M.; Agnew, D.C.; Hudnut, K.W.; Avouac, J.-P.; Natawidjaja, D.H. Uplift and subsidence associated with the great Aceh-Andaman earthquake of 2004. *J. Geophys. Res. Space Phys.* **2006**, *111*, 02407. [CrossRef]
19. Subarya, C.; Chlieh, M.; Prawirodirdjo, L.; Avouac, J.-P.; Bock, Y.; Sieh, K.; Meltzner, A.J.; Natawidjaja, D.H.; McCaffrey, R. Plate-boundary deformation associated with the great Sumatra–Andaman earthquake. *Nat. Cell Biol.* **2006**, *440*, 46–51. [CrossRef] [PubMed]
20. Sihombing, Y.I.; Adityawan, M.B.; Chrysanti, A.; Widyaningtias; Farid, M.; Nugroho, J.; Kuntoro, A.A.; Kusuma, M.A. Tsunami Overland Flow Characteristic and Its Effect on Palu Bay Due to the Palu Tsunami 2018. *J. Earthq. Tsunami* **2019**, *14*. [CrossRef]

21. Monecke, K.; Templeton, C.K.; Finger, W.; Houston, B.; Luthi, S.; McAdoo, B.G.; Meilianda, E.; Storms, J.E.; Walstra, D.J.; Amna, R.; et al. Beach ridge patterns in West Aceh, Indonesia, and their response to large earthquakes along the northern Sunda trench. *Quat. Sci. Rev.* **2015**, *113*, 159–170. [CrossRef]
22. Monecke, K.; Meilianda, E.; Walstra, D.-J.; Hill, E.M.; McAdoo, B.G.; Qiu, Q.; Storms, J.E.; Masputri, A.S.; Mayasari, C.D.; Nasir, M.; et al. Postseismic coastal development in Aceh, Indonesia—Field observations and numerical modeling. *Mar. Geol.* **2017**, *392*, 94–104. [CrossRef]
23. Meilianda, E.; Pradhan, B.; Syamsidik; Comfort, L.K.; Alfian, D.; Juanda, R.; Syahreza, S.; Munadi, K. Assessment of post-tsunami disaster land use/land cover change and potential impact of future sea-level rise to low-lying coastal areas: A case study of Banda Aceh coast of Indonesia. *Int. J. Disaster Risk Reduct.* **2019**, *41*, 101292. [CrossRef]
24. Leone, F.; Lavigne, F.; Paris, R.; Denain, J.-C.; Vinet, F. A spatial analysis of the December 26th, 2004 tsunami-induced damages: Lessons learned for a better risk assessment integrating buildings vulnerability. *Appl. Geogr.* **2011**, *31*, 363–375. [CrossRef]
25. Kaushik, H.B.; Jain, S.K. Impact of Great December 26, 2004 Sumatra Earthquake and Tsunami on Structures in Port Blair. *J. Perform. Constr. Facil.* **2007**, *21*, 128–142. [CrossRef]
26. Tobita, T.; Iai, S.; Banta, C.; Wimpie, A. Reconnaissance report of the 2004 great sumatra-andaman, Indonesia, Earthquake: Damage to geotechnical works in Banda Aceh and Meulaboh. *J. Nat. Disaster Sci.* **2006**, *28*, 35–41.
27. Jalil, A.; Fathani, T.F.; Satyarno, I.; Wilopo, W. A study on the liquefaction potential in banda aceh city after the 2004 sumatera earthquake. *Int. J.* **2020**, *18*, 147–155.
28. Natawidjaja, D.H.; Triyoso, W. The sumatran fault zone—From source to hazard. *J. Earthq. Tsunami* **2007**, *1*, 21–47. [CrossRef]
29. BAPPENAS. Scientific Basis: Analysis and Projection Sea Level Rise and Extreme Weather Event Report. In *ICCSR Report*; Ministry for National Development Planning: Lusaka, Zambia, 2010; p. 89.
30. Anh, N.Q.D.; Tanaka, H.; Tinh, N.X.; Viet, N.T. Sand spit morphological evolution at tidal inlets by using satellite images analysis: Two case studies in Vietnam. *J. Sci. Technol. Civ. Eng. (STCE) NUCE* **2020**, *14*, 17–27. [CrossRef]
31. Kombiadou, K.; Costas, S.; Carrasco, A.R.; Plomaritis, T.A.; Ferreira, Ó.; Matias, A. Bridging the gap between resilience and geomorphology of complex coastal systems. *Earth Sci. Rev.* **2019**, *198*, 102934. [CrossRef]
32. Goslin, J.; Clemmensen, L.B. Proxy records of Holocene storm events in coastal barrier systems: Storm-wave induced markers. *Quat. Sci. Rev.* **2017**, *174*, 80–119. [CrossRef]
33. Nott, J.; Forsyth, A.; Rhodes, E.; O'Grady, D. The origin of centennial- to millennial-scale chronological gaps in storm emplaced beach ridge plains. *Mar. Geol.* **2015**, *367*, 83–93. [CrossRef]
34. Masselink, G.; van Heteren, S. Response of wave-dominated and mixed energy barriers to storms. *Mar. Geol.* **2014**, *352*, 321–347. [CrossRef]
35. Sallenger, A.H.S. Storm impact scale for barrier island. *J. Coast. Res.* **2000**, *16*, 890–895.
36. Brantley, S.T.; Bissett, S.N.; Young, D.R.; Wolner, C.W.V.; Moore, L.J. Barrier Island Morphology and Sediment Characteristics Affect the Recovery of Dune Building Grasses following Storm-Induced Overwash. *PLoS ONE* **2014**, *9*, e104747. [CrossRef]
37. Long, A.J.; Waller, M.; Plater, A. Coastal resilience and late Holocene tidal inlet history: The evolution of Dungeness Foreland and the Romney Marsh depositional complex (U.K.). *Geomorphology* **2006**, *82*, 309–330. [CrossRef]
38. Stephan, P.; Suanez, S.; Fichaut, B. Long-, mid- and short-term evolution of coastal gravel spits of Brittany, France. In *Sand and Gravel Spits*; Randazzo, N., Jackson, D., Cooper, A., Eds.; Springer: Basel, Switzerland, 2015; pp. 275–288.
39. Morton, R.A.; Sallenger, A.H.S. Morphological impacts of extreme storms on sandy beaches and barriers. *J. Coast. Res.* **2003**, *19*, 560–573.
40. Sallenger, A.H.S.; Wright, C.W.; Howd, P.; Doran, K.; Guy, K. Extreme Coastal Changes on the Chandeleur Islands, Louisiana, During and After Hurricane Katrina. In *U.S. Geological Survey Scientific Investigations Report*; U.S. Geological Survey: Reston, VA, USA, 2009; pp. 27–36.
41. Woodroffe, C.D. The Natural Resilience of Coastal Systems: Primary Concepts. In *Managing Coastal Vulnerability*; McFadden, L., Penning-Rowsell, E., Nicholls, R.J., Eds.; Elsevier: Amsterdam, The Netherlands, 2007; pp. 45–60.
42. Riggs, S.R.; Cleary, W.J.; Snyder, S.W. Influence of inherited geologic framework on barrier shoreface morphology and dynamics. *Mar. Geol.* **1995**, *126*, 213–234. [CrossRef]
43. Hurukawa, N.; Wulandari, B.R.; Kasahara, M. Earthquake History of the Sumatran Fault, Indonesia, since 1892, Derived from Relocation of Large Earthquakes. *Bull. Seism. Soc. Am.* **2014**, *104*, 1750–1762. [CrossRef]
44. Kanagaratnam, U.; Schwarz, A.M.; Adhuri, D.; Dey, M.M. Mangrobe rehabilitation in West Coast of Aceh—Issues and perspectives. *NAGA WorldFish Cent. Q.* **2006**, *29*, 10–18.
45. Waltham, T. The Asian Tsunami disaster, December 2004. *Geol. Today* **2005**, *21*, 22–26. [CrossRef]
46. Syamsidik, S.; Oktari, R.S.; Munadi, K.; Arief, S.; Fajri, I.Z. Changes in coastal land use and the reasons for selecting places to live in Banda Aceh 10 years after the 2004 Indian Ocean tsunami. *Nat. Hazards* **2017**, *88*, 1503–1521. [CrossRef]
47. Al'ala, M.; Rasyif, T.M.; Fahmi, M. Numerical simulation of ujong seudeun land separation caused by the 2004 indian ocean tsunami, aceh-indonesia. *Sci. Tsunami Hazards* **2015**, *34*, 159–172.
48. Tursina; Syamsidik, S. Numerical simulations of land cover roughness influence on tsunami inundation in Ulee Lheue Bay, Aceh-Indonesia. In *IOP Conference Series: Earth and Environmental Science*; IOP Publishing: Bristol, UK, 2017; Volume 56, p. 12009.
49. Dominey-Howes, D.; Papathoma, M. Validating a Tsunami Vulnerability Assessment Model (the PTVA Model) Using Field Data from the 2004 Indian Ocean Tsunami. *Nat. Hazards* **2007**, *40*, 113–136. [CrossRef]

50. Dougherty, A.J.; Choi, J.-H.; Dosseto, A. Prograded Barriers + GPR + OSL = Insight on Coastal Change over Intermediate Spatial and Temporal Scales. *J. Coast. Res.* **2016**, *75*, 368–372. [CrossRef]
51. Van Maanen, B.; Nicholls, R.J.; French, J.R.; Barkwith, A.; Bonaldo, D.; Burningham, H.; Murray, A.B.; Payo, A.; Sutherland, J.; Thornhill, G.D.; et al. Simulating mesoscale coastal evolution for decadal coastal management: A new framework integrating multiple, complementary modelling approaches. *Geomorphology* **2016**, *256*, 68–80. [CrossRef]
52. Leont'Yev, I.O. Predicting shoreline evolution on a centennial scale using the example of the vistula (Baltic) spit. *Oceanology* **2012**, *52*, 700–709. [CrossRef]
53. Cowell, P.; Roy, P.; Jones, R. Simulation of large-scale coastal change using a morphological behaviour model. *Mar. Geol.* **1995**, *126*, 45–61. [CrossRef]
54. National Geophysical Data Center; NOAA; NCEI. NGDC/WDS Global Historical Tsunami Database. 2020. Available online: https://www.ngdc.noaa.gov/hazard/tsu_db.shtml (accessed on 30 October 2020). [CrossRef]
55. BMKG. *Catalogue of Significant and Destructive Earthquakes 1821–2017*; Pusat Gempa Bumi dan Tsunami Kedeputian Bidang Geofisika, BMKG: Jakarta, Indonesia, 2018.
56. Soloviev, S.L.; Go, C.N. *A Catalogue of Tsunamis on the Western Shore of the Pacific Ocean*; Academy of Sciences of the USSR, Ed.; Nauka Publishing House: Moscow, Russia, 1974; p. 439.
57. Lee, W.H.K.; Meyers, H.; Shimzaki, K. *Historical Seismograms and Earthquakes of the World*; Academic Press, Inc.: San Diego, CA, USA, 1988.
58. Kanamori, H.; Rivera, L.; Lee, W.H.K. Historical seismograms for unravelling a mysterious earthquake: The 1907 Sumatra Earthquake. *Geophys. J. Int.* **2010**, *183*, 358–374. [CrossRef]
59. Pentakota, S.; Seelanki, V.; Kolusu, S. Role of Andaman Sea in the intensification of cyclones over Bay of Bengal. *Nat. Hazards* **2018**, *91*, 1113–1125. [CrossRef]
60. Sahoo, B.; Prasad, K.B. Assessment on historical cyclone tracks in the Bay of Bengal, east coast of India. *Int. J. Climatol.* **2016**, *36*, 95–109. [CrossRef]
61. Siddiki, U.R.; Islam, M.N.; Ansari, M.N.A. Cyclonic track analysis using GIS over the Bay of Bengal. *Int. J. Appl. Sci. Eng. Res.* **2012**, *1*, 689–701.
62. CERC. Volume I: Technical Reference; Volume II: User's Guide. In *Automated Coastal Engineering System*; Department of the Army Waterway Experiment Station, Ed.; Corps of Engineers: Vicksburg, MS, USA, 1992.
63. Murty, T.S.; Rafiq, M. A tentative list of tsunamis in the marginal seas of the North Indian Ocean. *Nat. Hazards* **1991**, *4*, 81–83. [CrossRef]
64. Bilham, R.; Engdahl, R.; Feldl, N.; Satyabala, S.P. Partial and Complete Rupture of the Indo-Andaman Plate Boundary 1847–2004. *Seism. Res. Lett.* **2005**, *76*, 299–311. [CrossRef]
65. Pararas-Carayannis, G. Earthquake and Tsunami of June 26, 1941 in the Andaman Sea and the Bay of Bengal. 2005. Available online: http://www.drgeorgepc.com/Tsunami1941AndamanIslands.html (accessed on 30 October 2020).
66. Srivastava, K.; Kumar, R.K.; Swapna, M.; Rani, V.S.; Dimri, V.P. Inundation studies for Nagapattinam region on the east coast of India due to tsunamigenic earthquakes from the Andaman region. *Nat. Hazards* **2011**, *63*, 211–221. [CrossRef]
67. Murty, T. Storm surges—Meteorological ocean tides. In *Bulletin of the Fisheries Research Board of Canada*; National Research Council of Canada: Ottawa, ON, Canada, 1984.
68. Fearnley, S.; Miner, M.; Kulp, M.; Bohling, C.; Martinez, L.; Penland, S. Hurrican Impact and Recovery Shoreline Change Analysis and Historical Island Configuation. In *Sand Resources, Regional Geology, and Coastal Processes of the Chandeleur Islands Coastal System: An Evaluation of the Breton National Wildlife Refuge*; Lavoie, D., Ed.; U.S. Geological Survey: Reston, VA, USA, 2009; pp. 7–26.
69. Idris, Y.; Cummins, P.; Rusydy, I.; Muksin, U.; Syamsidik; Habibie, M.Y.; Meilianda, E. Post-Earthquake Damage Assessment after the 6.5 Mw Earthquake on December, 7th 2016 in Pidie Jaya, Indonesia. *J. Earthq. Eng.* **2019**, 1–18. [CrossRef]
70. Bennet, J.D.; Cameron, D.R.; Bridge, D.M.; Clarke, M.G.; Djunuddin, A.; Ghazali, S.A.; Thomson, S.J. *Geologic 1:250,000 Map of Banda Aceh Quadragle, Sumatra*; Geological Research and Development Centar (GDRC), Ed.; Direktorat Geologi: Bandung, Indonesia, 1983.
71. Ishihara, K.; Yoshimine, M. Evaluation of Settlements in Sand Deposits Following Liquefaction During Earthquakes. *Soils Found.* **1992**, *32*, 173–188. [CrossRef]
72. Volcano Discovery. Light mag. 4.7 Earthquake—Northern Sumatra, Indonesia on Friday, 8 April 1983. Available online: https://www.volcanodiscovery.com/earthquakes/quake-info/3801900/mag4quake-Apr-8-1983-northern-Sumatra-Indonesia.html (accessed on 30 October 2020).
73. McKinnon, E.E. Beyond Serandib: A note on Lambri at the northern tip of Aceh, Indonesia. In *Southeast Asia Program*; Cornell University: Ithaca, NY, USA, 1988; pp. 103–121.
74. Anthony, E.J. Patterns of Sand Spit Development and Their Management Implications on Deltaic, Drift-Aligned Coasts: The Cases of the Senegal and Volta River Delta Spits, West Africa. In *Coastal Research Library*; Randazzo, G., Jackson, D., Cooper, A., Eds.; Springer: Cham, Switzerland, 2015; p. 344.